STATISTICAL ANALYSES OF FRACTURE TOUGHNESS RESULTS FOR TWO IRRADIATED HIGH-COPPER WELDS*

Randy K. Nanstad, Donald E. McCabe, Fahmy M. Haggag,
Kimiko O. Bowman,† and Darryl J. Downing†

Metals and Ceramics Division
OAK RIDGE NATIONAL LABORATORY
Oak Ridge, Tennessee 37831-6151

CONF-900623--28

DE92 003282

ABSTRACT

The objectives of the Heavy-Section Steel Irradiation Program Fifth Irradiation Series were to determine the effects of neutron irradiation on the transition temperature shift and the shape of the K_{Ic} curve described in Sect. XI of the *ASME Boiler and Pressure Vessel Code*. Two submerged-arc welds with copper contents of 0.23 and 0.31% were commercially fabricated in 215-mm-thick plates. Charpy V-notch (CVN) impact, tensile, drop-weight, and compact specimens up to 203.2 mm thick [1T, 2T, 4T, 6T, and 8T C(T)] were tested to provide a large data base for unirradiated material. Similar specimens with compacts up to 4T were irradiated at about 288°C to a mean fluence of about 1.5×10^{19} neutrons/cm^2 (>1 MeV) in the Oak Ridge Research Reactor. Both linear-elastic and elastic-plastic fracture mechanics methods were used to analyze all cleavage fracture results and local cleavage instabilities (pop-ins). Evaluation of the results showed that the cleavage fracture toughness values determined at initial pop-ins fall within the same scatter band as the values from failed specimens; thus, they were included in the data base for analysis (all data are designated K_{Jc}).

---

*Research sponsored by the Office of Nuclear Regulatory Research, U.S. Nuclear Regulatory Commission, under Interagency Agreement DOE 1886-8109-8L with the U.S. Department of Energy under contract DE-AC05-84OR21400 with Martin Marietta Energy Systems, Inc.

†Engineering Physics and Mathematics Division.

The CVN results were analyzed by hyperbolic tangent and exponential curve fitting models to obtain the temperature shifts at the 41-J level. The temperature intervals associated with one standard deviation on energy were similar to that given for welds in *Regulatory Guide 1.99* (Rev. 2). A Weibull-based analysis validated the shift results from the tanh fits and showed that neutron fluence variations among the specimens were not significant to the observations. Using an exponential model, three-parameter nonlinear regression analyses of the K_{Jc} data showed that the intercept value of the ASME equation could be used. Equations of the same form were fit as mean curves and showed that the temperature shifts for K_{Jc} (at 100 MPa•$\sqrt{m}$) exceeded the CVN 41-J shifts for both welds. The same observation applies to the shifts of curves fit as lower boundaries to the data. Analyses of curve shape changes gave somewhat mixed results from the various mean curve fits, but curves constructed to lower bound all the data do indicate a substantial slope decrease, especially for the higher copper weld. The results were used to compare various procedures for shifting the ASME K_{Ic} curve to establish a suitable bounding curve for irradiated material.

KEY WORDS

Charpy V-notch impact toughness, compact specimens, copper content, elastic-plastic fracture, fracture toughness, irradiation, K_{Ic}, light-water reactors, lower bound, regulatory guide, nonlinear analyses, RT_{NDT}, submerged-arc welds, statistical analyses, standard deviation.

DISCLAIMER

Provisions for consideration of fracture toughness of the reactor pressure vessel are contained in *Title 10, Code of Federal Regulations, Part 50* (10CFR50) (ref. 1). Appendix G of 10CFR50 refers to the American Society of Mechanical Engineers (ASME) *Boiler and Pressure Vessel Code*[2] for determination of the reference nil-ductility temperature, RT_{NDT}. Appendix A, Sect. XI of the ASME Code contains fracture toughness (K_{Ic}) and crack arrest toughness (K_{Ia}) curves as a function of temperature (T) normalized to the RT_{NDT}, that is, $T - RT_{NDT}$. Both curves were constructed as lower bounds to their respective data bases.[3] The Heavy-Section Steel Irradiation (HSSI) Program at Oak Ridge National Laboratory (ORNL), funded by the U.S. Nuclear Regulatory Commission (NRC), includes the HSSI Fifth and Sixth Irradiation Series to investigate the effects of irradiation on the K_{Ic} and K_{Ia} transition curves, respectively, of reactor pressure vessel materials. The specific objectives are to evaluate the procedures for shifting those curves to account for irradiation effects and to evaluate the effects of radiation on the shape of each curve. Series 5 on the K_{Ic} curve shift is the subject of this paper while another paper in this volume by Iskander, Corwin, and Nanstad[4] discusses results from Series 6 on the K_{Ia} curve shift.

Description of Overall Program, Materials, and Irradiations

The Series 5 program, materials, specimen complement, and irradiation conditions have been described in detail previously.[5] Therefore, only a brief summary will be provided here. The program was designed to irradiate and test two different submerged arc welds to allow for verification of the K_{Ic} curve for irradiated materials to as high a K_{Ic} level as practicable. Weld wire was specially produced commercially for the program in one melt, and the melt was

split to allow for copper additions to one half. Thus, the chemical compositions of the two welds are as comparable as possible except for copper, as shown in Table 1. The welds were designated HSSI 72W and 73W (0.23 and 0.31% Cu). The welds were postweld heat treated at 607°C (1125°F) for 40 h, typical of that given commercial reactor vessels. Twelve separate specimen capsules were irradiated in the Oak Ridge Research Reactor at a nominal temperature of 288°C to fluences of about 1.5×10^{19} neutrons/cm^2 (>1 MeV). The specimen complement for irradiations included tensile, CVN, drop-weight, and compact specimens of 25.4-, 50.8-, and 101.6-mm (1-, 2-, and 4-in.) thickness [1T, 2T, and 4T C(T), respectively]. Additionally, to achieve K_{Ic} levels in the unirradiated condition comparable to the measuring capacity of the irradiated 4T specimen, unirradiated compact specimens of 152.4- and 203.2-mm thickness [6T and 8T C(T), respectively] were included in the program.

Test and Analysis Procedures

Details of the test and analysis procedures were presented in ref. 5 and will only be summarized here. Testing of CVN, tensile, and drop-weight specimens was conducted in accordance with applicable ASTM procedures. The specimen testing was a cooperative venture between ORNL and Materials Engineering Associates (MEA). All compact specimens (none of the specimens were side-grooved) were tested with a single specimen unloading compliance procedure, but no unloadings were performed prior to attainment of the 5% secant offset load so that K_{Ic} determinations would not be invalidated by unloadings. This was done to allow for acquisition of J-integral vs crack extension data for those specimens which sustain loading beyond the limits allowed in ASTM E 399, Standard

Test Method for Plane-Strain Fracture Toughness of Metallic Materials, for determination of a valid K_{Ic} in accordance with linear elastic fracture mechanics (LEFM). For those specimens which met the E 399 criteria for a valid K_{Ic}, the K_{Ic} value is used. If the plastic deformation was too extensive for a valid K_{Ic}, an elastic plastic fracture mechanics (EPFM) approach was adopted; a J-integral at the point of cleavage fracture, J_c, was determined and a critical value of stress intensity K_{Jc} was calculated from

$$K_{Jc}^2 = EJ_c \ , \qquad (1)$$

where E is Young's modulus. For the few specimens which exhibited essentially linear elastic test records, but did not meet the size requirements for a valid K_{Ic}, the elastically calculated provisional fracture toughness result, K_Q, was used. Because the data base includes results from both LEFM and EPFM calculations, all fracture toughness data have been designated K_{Jc}. Many of the irradiated compact specimens exhibited small cleavage instabilities (pop-ins) prior to the final cleavage instability. Determination of the significance of those events is an important element of the analyses and will be discussed.

Summary of Test Results

In the unirradiated condition, the two weld metals have very similar tensile properties. At room temperature, the 0.2% offset yield strengths are 500 and 493 MPa, while ultimate strengths are 609 and 604 MPa, for 72W and 73W, respectively. Irradiation exposure increased the yield strengths about 24 and 32%, while the ultimate strengths increased about 18 and 23%, for 72W and 73W,

respectively. The drop-weight nil-ductility transition (NDT) temperatures are -23°C for 72W and -34°C for 73W, and the RT_{NDT} of each weld is equal to its NDT. Figures 1 and 2 show the Charpy V-notch (CVN) impact test results for both welds in the unirradiated and irradiated conditions. The curves represent hyperbolic tangent fits and show the radiation-induced 41-J temperature shifts of 72 and 82°C, and upper-shelf decreases of 30 and 33% for 72W and 73W, respectively. All the changes are greater for the higher copper 73W weld. As shown in the figures, the mean curve for weld 73W exhibited a substantial shape change while that for 72W was much less. After adjusting the irradiated drop-weight NDT results for differences in neutron fluence, as detailed in ref. 5, the NDT temperature and CVN 41-J temperature shifts are very close; 69 vs 72°C for 72W, and 80 vs 82°C for 73W.

The results of fracture toughness tests for the unirradiated 72W and 73W welds are shown in Figs. 3 and 4, respectively. The dashed lines represent the limits of valid K_{Ic} measurements (according to E 399) for the larger specimens as a function of test temperature (the valid K_{Jc} values increase with decreasing temperature because the material yield strengths increase with decreasing temperature). The ASME K_{Ic} curve from Sect. XI is plotted relative to the RT_{NDT} of the material. As shown, all the data are on or above the K_{Ic} curves, and the curve is a good representation of a lower bound to the data for both welds. The 6T and 8T test temperatures were chosen based on Weibull analysis predictions made using data from smaller specimens that indicated the likelihood of achieving valid or very near valid K_{Ic} values. However, the large specimen results scatter above the K_{Ic} limits, except for a 6T pop-in result for 72W at 10°C. The irradiated results for 72W and 73W are shown in Figs. 5 and 6, respectively. The

solid curve in each case represents the ASME K_{Ic} curve for unirradiated material shifted upward in temperature by an amount equal to the CVN 41-J shift as specified by E 185. Two results (both cleavage pop-ins) for 72W and six results (two specimen failures and four pop-ins) for 73W fall below the shifted curve. A bounding curve with the same shape as the ASME curve shifted in temperature to bound all data, would indicate a fracture toughness shift of about 101°C for 73W, compared with the CVN 41-J shift of 82°C.

Analyses of Charpy Impact Test Results

Title 10. Code of Federal Regulations, Part 50 (10CFR50) includes provisions, by reference, for determination of the upward temperature shift of the RT_{NDT}. The 10CFR50 references ASTM Standard Practice for Conducting Surveillance Tests for Light Water-Cooled Nuclear Power Reactor Vessels (E 185) for determination of the shift in RT_{NDT}. The current E 185 procedures require a minimum of 12 CVN specimens to develop a full curve of CVN toughness versus test temperature with stated emphasis on concentration of testing near to the temperature at which the material achieves 30 ft-lb (41 J). The irradiated RT_{NDT} is determined by adding the temperature shift between the unirradiated and irradiated CVN curves at the 41-J (30-ft-lb) level (ΔTT_{30}) to the unirradiated RT_{NDT}.

Regulatory Guide 1.99 (Rev. 2) provides guidelines for calculating the effects of neutron radiation embrittlement for reactor vessels.[6] When two or more credible surveillance data sets are available, they may be used to determine

the adjusted reference temperature (ART) and the Charpy upper-shelf energy of the beltline materials. The ART is defined as follows:

$$\text{ART} = \text{Initial } RT_{NDT} + \Delta RT_{NDT} + \text{Margin} , \quad (2)$$

where the initial RT_{NDT} is the reference temperature for the unirradiated material, ΔRT_{NDT} is the temperature difference between the unirradiated and irradiated data sets measured at the 30-ft-lb (41-J) level, and "Margin" is defined as $2\sqrt{(\sigma_I^2 + \sigma_\Delta^2)}$. In the margin equation, σ_I (standard deviation for the initial RT_{NDT}) is generally defined as zero.* The σ_Δ (standard deviation for ΔRT_{NDT}) is 28°F (15.6°C) for welds, but σ_Δ may be defined as 14°F (7.8°C) when credible surveillance data are available. Because the ART is used as the basis for construction of the K_{Ic} curve for the applicable irradiated material, the relationship between the CVN 41-J temperature shift and the K_{Ic} temperature shift at 100 MPa•√m is of interest, as is the shape of the fracture toughness curve.

Various analyses of the CVN impact results were performed. It is common to fit CVN impact data with either hyperbolic tangent or exponential functions and both of these were used for this study. In both cases, the upper-shelf portion of the curve fit was made horizontal in one instance and allowed to have a slope in the second instance. The mean square error was used to compare the four fits for each weld. Although all four fits gave very similar 41-J shifts, the hyperbolic tangent with horizontal upper shelf gave the smallest mean square error; they are shown in Figs. 1 and 2. Using the hyperbolic tangent form, the

---

*Personal discussion with P. N. Randall, U.S. Nuclear Regulatory Commission, June 1990.

data were analyzed to obtain bounding curves based on one standard deviation of impact energy. Figures 7 and 8 show the results of these analyses. The temperature intervals between the mean and lower bounding curves at the 41-J level for 72W and 73W, respectively, are about 13 and 11°C for the unirradiated data, and 11 and 18°C for the irradiated data. For the 41-J temperature shift, the temperature intervals associated with one standard deviation are about ±20 and ±22°C for welds 72W and 73W, respectively. The figures also show that the temperature shifts and confidence intervals are greater at the 68-J level; this is especially so for 73W which indicates a greater irradiation-induced change in the curve shape than for 72W. The 68-J temperature shifts and associated temperature intervals are 83 ± 20°C and 105 ± 27°C for 72W and 73W, respectively.

To evaluate the role, if any, of variations in neutron fluence and to place limits on the error of estimation of the 41-J temperature shift, a Weibull analysis was performed. The details of this procedure have been published separately.[7] In summary, however, it was assumed that the scale parameter in the Weibull distribution is a function of temperature (and neutron fluence for the irradiated Charpy V-notch data). In the data analysis, the distribution selection technique of Kent and Quesenberry[8] was used and the Weibull distribution was selected by that technique as the best distribution for these data, at least in the transition region. An inverse regression technique was then used to solve for the temperature corresponding to an impact energy of 41 J. To obtain error bounds on this estimate, the parameters of the equation describing the scale parameter were resampled assuming a normal distribution and the inverse regression repeated several times. This procedure leads to several

estimates of the temperature and the variance of these values were used to give bounds on the error of estimation. The 41-J temperature shifts from these analyses were similar to the shifts determined with the hyperbolic tangent fits. The standard errors range from ±3.0 to ±5.3°C with the higher values obtained with neutron fluence included as an additional predictor variable in the model (values of ±3.2 and ±3.8°C for 72W and 73W, respectively, were obtained when fluence is not included). Thus, estimates of the 95% confidence prediction on the 41-J shifts range from ±6.0 to ±10.6°C. The major contribution of these analyses is that a statistically defensible method for calculating error on the 41-J temperature shift was described. Another important result of these analyses is that differences in neutron fluence among the irradiated specimens did not substantially affect the results; this observation is particularly important when considering the effects of irradiation on curve shape.

Examination of the Fracture Toughness Results

Regarding the fracture toughness results, the first step was to evaluate the data to establish the data base appropriate for statistical analyses. The preponderance of cleavage pop-ins in the irradiated specimens required examination of those results. Out of 156 unirradiated compact specimens, only two exhibited pop-ins. For the 110 irradiated specimens, however, 28 specimens exhibited a total of 39 pop-ins. The analysis of those results included a determination of the significance of the pop-in events, the effects of pop-ins on final specimen fracture, and the appropriate method for determination of fracture toughness. When the pop-in event is relatively large or there are multiple pop-ins in the same specimen, it seems likely that the determination of

the J-integral at final fracture using the area under the curve method would be erroneous due to the periodic jumps in displacement being credited as plastic deformation in the crack tip region. Although there are various suggested schemes for determination of fracture toughness in the presence of pop-ins, and for determination of significant pop-ins, there is not a rigorously developed computational practice. Likewise, there is not even a standard method for determination of cleavage toughness using elastic-plastic analyses. The relationship between a cleavage pop-in in a laboratory test specimen and cleavage fracture in a large structure such as a reactor pressure vessel is certainly difficult to quantify. It is for these reasons that only the initial pop-in was used herein to determine cleavage fracture toughness for those specimens exhibiting pop-ins. Pop-ins of any size representing a cleavage event in the specimen were considered significant.

Figure 9 shows a plot of cleavage fracture toughness for weld 72W in the irradiated condition. Each datum plotted represents one test specimen. The results are plotted to allow for direct comparison of fracture toughness from specimens with pop-ins with those which failed in cleavage without exhibiting pop-ins at the same test temperature (the abscissa is not scaled). As shown, the pop-in results fit generally within the scatter bands of the fracture results and the lowest values are mixed between pop-ins and fracture results. These results suggest that cleavage pop-ins are significant in that they indicate propensity for cleavage fracture in the test specimen. Similar results were observed for weld 73W.

Analyses of Fracture Toughness Results

The K_{Ic} curve in Sect. XI of the ASME Code is a lower boundary to the data used for its development.[3] The equation for that curve is:

$$K_{Ic} = 36.48 + 22.783 \exp[0.036(T - RT_{NDT})] , \quad (3)$$

where T is temperature (°C), RT_{NDT} is the value of RT_{NDT} (°C) for the specific material, and K_{Ic} is in MPa•√m.

Three-parameter nonlinear regression analyses were performed for 72W and 73W in both the unirradiated and irradiated conditions. The simple exponential form of the ASME K_{Ic} curve was used for these analyses. Using the three-parameter equations, the fracture toughness 100 MPa•√m temperature shifts are about 94 and 100°C for 72W and 73W, respectively. Various intercept values were obtained but statistical analyses revealed that they did not differ significantly from the ASME value of 36.48, but the standard errors for those intercept estimates were very large relative to the values of the intercepts. Furthermore, the estimates of the constants in the equation for 72W and 73W unirradiated data were within one standard deviation of each other, implying that the model for 72W and 73W may be the same. Based on the above results, the intercept value was fixed at 36.48 and the model used for subsequent analyses is as follows:

$$K_{Jc} = 36.48 + b*\exp(c*T) + e , \quad (4)$$

where b and c are fitting constants, T is temperature (°C), and e is the error estimate.

The subsequent two-parameter nonlinear regression analyses gave results very similar to those obtained with the three-parameter model, except that the standard errors were much less. Table 2 gives the results of those analyses and shows each fitting constant and associated standard deviation for each case examined. For the combined data, T becomes ($T - RT_{NDT}$) where RT_{NDT} is -23°C for 72W and -34°C for 73W for the unirradiated case. For the irradiated case, the Charpy 41-J temperature shifts of 72 and 82°C were added to the RT_{NDT} values for 72W and 73W, respectively. Using these mean curve fits, the fracture toughness 100 MPa•$\sqrt{m}$ temperature shifts are about 94 and 100°C for 72W and 73W, respectively, the same results obtained from the three-parameter nonlinear regression analyses. For the case of the combined data, normalized to the RT_{NDT}, the difference between the unirradiated and irradiated curves at 100 MPa•$\sqrt{m}$ is 20°C. This difference reflects the fact that the fracture toughness shifts for both welds are greater than the Charpy 41-J shifts by about 20°C for both 72W and 73W, respectively.

In order to better examine changes in shape of the curve, the data were translated by the intercept and a multiplicative error was considered, instead of an additive error, so that the model could be linearized. The resulting model used is as follows:

$$\ln(K-36.48) = a + c*T + e \quad . \qquad (5)$$

Table 3 gives the results of those analyses and shows each fitting constant and associated standard deviation for each case examined. Based on those equations, the fracture toughness 100-MPa•√m temperature shifts are about 83 and 99°C for 72W and 73W, respectively. Because the slopes are different, however, the shift increases with increasing fracture toughness. The fitting constant "c" represents the slope of the linear regression curve. To determine the temperature interval associated with one standard deviation on fracture toughness and to determine the standard error on prediction of the 100-MPa•√m temperature shift, the constant "c" was averaged between the unirradiated and irradiated results for each weld. The 100-MPa•√m temperature shifts from those equations are 84 and 100°C for 72W and 73W, respectively. Figures 10 and 11 show the curve fits obtained for 72W and 73W, respectively. The plots also show upper- and lower-bounding curves representing one standard deviation on fracture toughness. With decreasing test temperature, the temperature interval about the mean curve increases, but the fracture toughness interval is about the same. Using the temperature intervals between the means and lower bounding curves only results in associated standard deviations of 37 and 30°C for 72W and 73W, respectively. These results compare with Charpy impact associated standard deviations of 20°C for 72W and 22°C for 73W. Thus, the temperature intervals associated with one standard deviation were greater for the fracture toughness data than for the Charpy data. Regarding the standard error on temperature shift predictions, however, the 95% confidence values are about ±6 and ±5°C for the fracture toughness shifts compared to about ±3 and ±4°C for the Charpy shifts for 72W and 73W, respectively.

The 95% confidence intervals for the constant "c" (slope of the curve) were calculated and the results are also given in Table 3 for both welds in both conditions and for the combined data set in the unirradiated condition. As shown by the values of "c," the curve slopes for the irradiated data are somewhat lower than for the unirradiated data for both the individual welds and for the combined data sets. Most of the values of "c" are included in any of the asymptotic confidence intervals, however, implying a small statistical difference between them. With temperature normalized to the RT_{NDT}, the curves for the irradiated data are displaced upward in temperature as shown in Fig. 12 for weld 73W. At K_{Jc} values of 50, 100, and 200 MPa•√m, the differences are 12.0, 17.4, and 20.6°C. The fact that there is a temperature offset between the two curves simply reflects the earlier observation that the shift in fracture toughness is greater than the CVN shift. However, the increasing temperature offset between the two curves with increasing K_{Jc} reflects the change in curve shape. If there was no curve shape change, the offset would be constant. The difference between the normalized unirradiated and irradiated curves for weld 73W increases about 8.6°C over the K_{Jc} range from 50 to 200 MPa•√m. The corresponding change for 72W is 5.3°C, indicating a greater change in slope for the higher copper weld. Similarly, the corresponding change between the ASME K_{Ia} and K_{Ic} curves is 12.1°C.

It is interesting that simple manual construction of lower bounding curves to the data result in measured temperature shifts within a few degrees of those determined by the various mean fits. Moreover, elimination of the cleavage pop-in results from the data base would, for 72W, result in a temperature shift comparable to that for the CVN data while, for 73W, the temperature shift would still be about 100°C compared to the 82°C shift for the CVN data. Also, manually

constructed curves, especially for 73W, suggest a shape change for the lower-bound curves.

Size Effects and Stable Ductile Tearing

Preliminary examinations were performed regarding effects of specimen thickness on transition temperature behavior and on precleavage stable ductile tearing. Figure 13 shows a plot of K_{Jc} vs precleavage stable ductile tearing for the unirradiated weld 73W. The ductile tearing was measured on the specimen fracture surface with a digital toolmaker's microscope. The data are plotted without regard to test temperature and, as shown, form a resistance curve (R-curve) of fracture toughness vs ductile tearing prior to cleavage. There is no apparent effect of specimen thickness on the R-curve. The same result was observed with weld 72W.

Regarding size effects on the K_{Jc} fracture toughness as a function of test temperature, the data were separated according to specimens size and simple linear fits were performed using the exponential model,

$$K_{Jc} = C*\exp(D*T_R) \quad , \tag{6}$$

where C and D are constants of fit and T_R (°C) is equal to $T - RT_{NDT}$. Three-parameter nonlinear fits were also performed with the intercept value set to zero, but the results were not significantly different than those obtained using the linear fits. Combining the 72W and 73W data gave the following equations for the 1T, 2T, and 4T specimens:

Specimen Size	Linear Fit
1T	$K_{Jc} = 150.9 \exp(0.0123*T)$
2T	$K_{Jc} = 134.5 \exp(0.0125*T)$
4T	$K_{Jc} = 119.5 \exp(0.0116*T)$

For a K_{Jc} value of 100 MPa•√m, the corresponding temperatures ($T - RT_{NDT}$) are -33, -24, and -15°C for the 1T, 2T, and 4T specimens, respectively. Figure 14 provides a graphical comparison of the curve fits and shows the fracture toughness transition temperature increasing with increasing specimen thickness. The 95% confidence bounds range from about ±5°C for the 1T specimens to about ±10°C for the 4T specimens. The 6T and 8T specimens were not included in this comparison because of the paucity of data. Thus, the confidence bounds for the 1T and 4T specimens do not overlap indicating a statistically significant effect of specimen size. Preliminary Weibull analyses show similar results. Similar exponential analyses of the data base excluding specimens which experienced more than 0.2-mm stable tearing (exclusive of blunting) prior to cleavage showed similar results. It appears, then, that the effect of specimen size on the cleavage fracture toughness results is due to crack tip constraint but not precleavage ductile tearing.

Weibull-Based Analysis

Wallin[9] has developed an analysis procedure which involves fitting a Weibull distribution to the fracture toughness data at each temperature. Wallin performs a size adjustment which is derived from a fixed Weibull slope concept. The adjusted fracture toughness from a specimen larger than 1T will be increased.

He determined that the Weibull slope is always equal to four, which is near the value that makes the Weibull and normal distributions (Weibull slope of 3.25) almost indistinguishable from one another. By fixing the shape parameter, one then estimates the scale parameter (the K_{Jc} fracture toughness at the 0.632 failure probability level) at each temperature. The results are then fit with an exponential equation using temperature normalized to the 100 MPa•√m temperature as the independent variable. To obtain bounding curves, then, one can fit the exponential to the desired percentile, e.g., the five or one percentile.

The Wallin procedure was used to analyze the fracture toughness data for 72W and 73W. Although this analysis indicated that a shape parameter (Weibull slope) of 3.25 and the normal distribution may be a better choice, the equation that employs the Wallin slope was used. For the 1T data in this study, an intercept value of 24.41 was obtained with a standard error of 26.33. Since that result is not statistically different from the value of 31 used by Wallin, the intercept was fixed at 31 and the data were fit with an exponential to obtain,

$$K_{0.632} = 31 + 76.65*\exp[0.0166*(T - T_o)] \ , \qquad (7)$$

where T is test temperature, and T_o is the temperature at 100 MPa•√m. Equation (7) was not found to be statistically different from that given by Wallin. In the Wallin equation, the "b" coefficient is 77, while the "c" coefficient is 0.019. Likewise, the ten and five percentile results were fit and the estimated equations are:

$$K_{0.10} = 25.33 + 34.88*\exp[0.0177*(T - T_o)] \quad , \tag{8}$$

$$K_{0.05} = 25.24 + 24.55*\exp[0.019*(T - T_o)] \quad , \tag{9}$$

Figure 15 shows a plot of all the unirradiated and irradiated data adjusted for size using Wallin's procedure as well as the Wallin curve and the five percentile curve from Eq. (9). The five percentile curve (≈95% confidence) just provides a bound to all the data; the ten percentile curve from Eq. (8) did not bound all the data. The size adjustment has increased the scatter because some of the large specimens gave larger fracture toughness values than the 1T specimens and the adjustment procedure that predicts the equivalent toughness for 1T size specimens assumes the opposite case. Furthermore, it appears that substantially more than 63.2% of the results fall below the curve based on Wallin's analysis.

Figures 16 and 17 show plots of the irradiated fracture toughness data and various curves for 72W and 73W, respectively. The ASME K_{Ic} curve is shown for the unirradiated condition and for the irradiated condition after shifting the curve upward in temperature equal to the Charpy 41-J shift (ΔTT_{41}). The dashed curves labeled 1 through 3 represent different methods for shifting the K_{Ic} curve. The curve labeled 4 represents the ASME K_{Ia} curve shifted upward in temperature equal to the Charpy 41-J shift. The curve labeled 5 is the 5 percentile curve produced using the method of Wallin. For 72W, the data are bounded by the ΔTT_{41} + Margin curve and the ΔK_{Jc} curve, but neither of those curves quite bound all the data for 73W. The margin is 15.6°C as defined in *Regulatory Guide 1.99* (Rev. 2) assuming credible surveillance data. In both cases, applying the margin to the ΔK_{Jc} results provides an adequate bound. The

K_{Ia} curve is shown to allow for comparison of that curve with the shifted K_{Ic} curves, especially regarding curve shape in view of the observation that the irradiated K_{Jc} curves for these two welds appear to have exhibited some shape change after irradiation.

Summary and Discussion

The two primary objectives of this study were to determine the effects of neutron irradiation on the fracture toughness temperature shift and the shape of the fracture toughness (K_{Ic}) curve for two submerged-arc welds with copper contents of 0.23 and 0.31%. As shown in Fig. 9, the fracture toughness values from small cleavage pop-ins suggest that the pop-ins observed in this study are significant in that they indicate propensity for cleavage fracture in the test specimen. Regarding the irradiation-induced temperature shift, statistical analyses and curve fitting showed that the temperature shifts at a fracture toughness of 100 MPa•√m were greater than those at a Charpy energy of 41 J for both welds. The shifts and the differences between the Charpy and fracture toughness shifts were greater for the higher copper weld. The amounts of the 100-MPa•√m shifts were dependent on the fitting technique; the three-parameter and two-parameter nonlinear fits gave shifts of about 94 and 100°C, while the linearized two-parameter fit gave shifts of about 83 and 99°C for 72W and 73W, respectively. Thus, for weld 72W, the 100-MPa•√m shift is from 11 to 22°C greater than the Charpy shift, while it is about 18°C greater for weld 73W.

Furthermore, using the linear fits, the temperature intervals associated with one standard deviation on the fracture toughness data, 37 and 30°C, are

greater than those for the Charpy impact data, 20 and 22°C for 72W and 73W, respectively. Table 4 summarizes these observations. As shown in the table, using the linear fits, the 100-MPa•√m temperature shifts, defined as the mean shift plus one standard deviation on the data, are 120 and 129°C; these values can be compared with similarly defined Charpy 41-J temperature shifts of 92 and 102°C, for 72W and 73W, respectively. The Charpy 68-J transition temperature shifts are in much better agreement with the fracture toughness shifts than are the 41-J shifts, but this observation is presently regarded as fortuitous in the absence of other similar experimental evidence.

In a study of irradiation-induced Charpy and fracture toughness shifts, Hiser[10] also used a mean curve-fitting technique and compared the reported results from plates, forgings, and welds. The analyses revealed that, for fracture toughness shifts relative to those for Charpy impact, plates were about 15°C greater, forgings were about 24°C greater, and welds were about the same. The overall average comparison was that the 100-MPa•√m fracture toughness shifts were about 10°C greater than the Charpy 41-J shifts. The report also showed that one standard deviation temperature intervals between the means and lower boundary curves ranged from about 11 to 64°C, with an overall value of about 32°C. As noted in the report, many of the fracture toughness curves were developed with six or even fewer data, thus, the uncertainties in those cases would be quite high. Hence, the overall observations concerning fracture toughness shifts are generally similar to those of this study.

Regarding the shape of the fracture toughness curve, the results from curve-fitting data are somewhat mixed. That is, the three-parameter and

two-parameter nonlinear mean fits show greater shifts at 100 MPa•√m than at 200 MPa•√m, indicating no decrease in slope or flattening of the curves. The linearized two-parameter fits, however, do indicate some decreases in the slopes, with the higher copper 73W weld exhibiting a somewhat greater change than for 72W. Using a 95% confidence criterion, however, the statistical significance of those changes is marginal. On the other hand, curves constructed to lower bound all the data do indicate a substantial slope decrease, especially for weld 73W. Because the ASME K_{Ic} curve is a lower-bound curve for the data used for its construction, this latter observation is more important. The five percentile curve from the Wallin procedure bounds all the data, but the curve has a substantially lower slope than the ASME K_{Ic} curve and appears to be overly conservative at fracture toughness levels above about 100 MPa•√m. Of course, concerns about curve shape changes can be accounted for by applying large enough shifts to the K_{Ic} curve, but such a practice begs the issue of how good accuracy can be developed when the trend line (curve shape) does not fit the real fracture toughness trend for the irradiated condition.

The data in the present case indicate that the K_{Ic} curve shifted by the 41-J Charpy V-notch plus "margin" would not have lower bounded a larger data base, and more margin adjustment is needed. The difficulty is that added margin to cover high toughness K_{Jc} values will result in overconservatism in the lower transition region. Therefore, shallower curves such as the five percentile curve of Wallin or the K_{Ia} curve deserve consideration. A reasonable argument can be made for use of the K_{Ia} curve <u>shape</u> on the basis that irradiation damage tends to increase material strength and consequently reduce the strain rate sensitivity of reactor pressure vessel steels such that K_{Ic} values tend toward agreement with

K_{Ia} values. Preliminary observations from the HSSI Sixth Irradiation Series on crack-arrest toughness indicate no irradiation-induced curve shape changes in the K_{Ia} curve.[4] One consideration, then, would be the use of the K_{Ia} curve shape to describe the irradiated K_{Ic} curve for materials which exhibit irradiation-induced toughness shifts above some prescribed amount.

Regarding specimen size effects, the exponential curve fits to the unirradiated data separated by specimen size (1T, 2T, and 4T) indicated a size effect on the fracture toughness results with smaller specimens showing higher average toughness. It is also true, however, that the smaller specimens often exhibit the lower toughness values at a given temperature. An important result was shown in Fig. 13 in that there was no apparent size effect on the resistance curve of fracture toughness vs precleavage ductile tearing. These results indicate that size effects on the fracture toughness results were due to crack-tip constraint, but not precleavage ductile tearing.

As discussed earlier, the cleavage pop-ins observed in this study were judged to be significant relative to structural integrity of the test specimens. It is not clear what the relationship is between those pop-ins and structural integrity in a reactor pressure vessel. To some degree, the quantitative results from this study are dependent on the inclusion of those pop-ins. However, exclusion of those results from the data base would not remove the observed differences between the fracture toughness and Charpy shifts. Resolution of this issue is beyond the scope of this paper.

Conclusions

The principal conclusions drawn from this study are as follows:

1. Cleavage pop-ins were significant in that they indicate propensity for cleavage fracture in the test specimen.

2. Fracture toughness temperature shifts at 100 MPa•√m are about -12 and 18°C greater than the corresponding Charpy 41-J shifts, but are similar to the Charpy 68-J shifts.

3. The temperature intervals associated with one standard deviation on the fracture toughness results are greater than the corresponding intervals for the Charpy results. Therefore, the mean 100-MPa•√m shifts plus one standard deviation temperature interval are substantially greater than the corresponding shifts for the Charpy results.

4. The Charpy 41-J shifts plus the margin (one standard deviation) in *Regulatory Guide 1.99* (Rev. 2) do not bound all the fracture toughness data.

5. Nonlinear and linear mean curve fits to the fracture toughness data provide mixed results regarding irradiation-induced curve shape changes, but the linearized two-parameter fits did indicate curve shape changes for both welds with the change being greater for weld 73W (0.31% Cu) than that for weld 72W (0.23% Cu). Curves constructed as lower boundaries to the data indicate curves of substantially lower slopes.

Acknowledgments

The authors acknowledge Julia L. Bishop for preparation of the draft manuscript, and David J. Alexander and Gene M. Goodwin for their helpful reviews. Program management support from William R. Corwin and financial support from the U.S. Nuclear Regulatory Commission, Michael E. Mayfield and Alfred Taboada, former and current technical monitors, respectively, are much appreciated. This research was sponsored by the Office of Nuclear Regulatory Research, U.S. Nuclear Regulatory Commission, under interagency agreement DOE 1886-8109-8L with the U.S. Department of energy under contract DE-AC05-84OR21400 with Martin Marietta Energy Systems, Inc.

References

1. *Title 10, Code of Federal Regulations, Part 50*, U.S. Government Printing Office, Washington, D.C., January 1987.

2. *ASME Boiler and Pressure Vessel Code, An American National Standard*, American Society of Mechanical Engineers, New York, 1986.

3. *ASME Boiler and Pressure Vessel Code, An American National Standard*, Sect. XI, Appendix A, American Society of Mechanical Engineers, New York, 1986.

4. S. K. Iskander, W. R. Corwin, and R. K. Nanstad, "Effects of Irradiation on Crack-Arrest Toughness of Two High-Copper Welds," *Effects of Radiation on Materials: 15th International Symposium, ASTM STP ____*, R. E. Stoller and A. S. Kumar, Eds., American Society for Testing and Materials, Philadelphia, 1990, pp. ___-___.

5. R. K. Nanstad, D. E. McCabe, B. H. Menke, S. K. Iskander, and F. M. Haggag, "Effects of Radiation on K_{Ic} Curves for High Copper Welds," *Effects of Radiation on Materials: 14th International Symposium (Volume II), ASTM STP 1046*, N. H. Packan, R. E. Stoller, and A. S. Kumar, Eds., American Society for Testing and Materials, Philadelphia, 1990, pp. 214-233.

6. "Radiation Embrittlement of Reactor Vessel Materials," *Regulatory Guide 1.99* (Rev. 2), U.S. Nuclear Regulatory Commission, Washington, D.C., May 1988.

References (Continued)

7. D. J. Downing, F. M. Haggag, and R. K. Nanstad, "Estimating Charpy Transition Temperature Shift Using Weibull Analysis," *Int. J. Pres. Ves. & Piping* 44, 241-54 (1990).

8. J. Kent and C. P. Quesenberry, "Selecting Among Probability Distributions Used in Reliability," *Technometrics*, Vol. 24, 1982, pp. 59-65.

9. K. Wallin, "The Scatter in K_{Ic}-Results," *Engineering Fracture Mechanics*, Vol. 19, No. 6, 1984, pp. 1085-1093.

10. A. L. Hiser, *Correlation of Irradiation-Induced Transition Temperature Decreases from C_v and K_{Jc}/K_{Ic} Data*, NUREG/CR-5494 (MEA-2377), Materials Engineering Associates, Inc. Lanham, Md., March 1990.

Table 1. Chemical composition of the two submerged-arc welds, 72W and 73W, in the HSSI Fifth Irradiation Series

Material	Composition, wt %									
	C	Mn	P	S	Si	Cr	Ni	Mo	Cu	V
72W	0.093	1.60	0.006	0.006	0.44	0.27	0.60	0.58	0.23	0.003
73W	0.098	1.56	0.005	0.005	0.45	0.25	0.60	0.58	0.31	0.003

Table 2. Summary of two-parameter nonlinear regression analyses of fracture toughness results for HSSI welds 72W and 73W

Weld	b[a]	σ(b)[a]	c[a]	σ(c)[a]
72W unirradiated	136.97	5.55	0.0149	0.0018
72W irradiated	28.07	7.43	0.0193	0.0029
73W unirradiated	168.83	5.87	0.0169	0.0012
73W irradiated	30.64	6.97	0.0173	0.0020
72W and 73W unirradiated	97.00	3.55	0.0158	0.0010
72W and 73W irradiated	71.81	5.99	0.0181	0.0021

[a] K_{Jc} = 36.48 + b*exp(C*T),
σ(b) = standard deviation on parameter b, and
σ(c) = standard deviation on parameter c, where
T is test temperature for individual data sets and
T = test temperature - RT_{NDT} for the combined data sets.
RT_{NDT} values for unirradaited 72W and 73W are -23°C and -34°C, respectively; RT_{NDT} values for irradiated 72W and 73W are 49°C and 48°C, respectively.

Table 3. Summary of linearized two-parameter exponential regression analyses of fracture toughness results for HSSI welds 72W and 73W

Weld	α	$\sigma(\alpha)$	c	$\sigma(c)$	Asymptotic 95% confidence intervals for parameter c	
					Lower	Higher
72W unirradiated	4.94	0.070	0.0197	0.0014	0.0169	0.0224
72W irradiated	3.33	0.087	0.0189	0.0011	0.0166	0.0212
73W unirradiated	5.20	0.054	0.0216	0.0010	0.0196	0.0236
73W irradiated	3.13	0.102	0.0201	0.0014	0.0173	0.0229

$\ln(K_{Jc} - 36.48) = \sigma + C * T$ and
$\sigma(\alpha)$ = standard deviation on parameter α,
$\sigma(c)$ = standard deviation on parameter c, where T is test temperature.

Table 4. Summary of irradiation-induced transition temperature shifts for HSSI welds 72W and 73W

Weld	Charpy 41-J shift (Charpy 68-J shift) (°C)				Fracture toughness 100 MPa•√m shift[a] (°C)			
	Mean	Temperature interval for 1σ	Total	Mean + margin[b]	Mean	Temperature interval for 1σ	Total	Mean + margin[b]
72W	72 (82)	20 (20)	92 (102)	87.6 (97.6)	83	37	120	98.6
73W	82 (105)	22 (27)	102 (132)	97.6 (120.6)	99	30	129	114.6

[a]Using linearized two-parameter fit.

[b]Margin for *Regulatory Guide 1.99* (Rev. 2) assuming credible surveillance data, 1σ = 15.6°C.

List of Figures

Fig. 1. Charpy V-notch impact energy vs test temperature for HSSI weld 72W in the unirradiated condition and following irradiation at 288°C to an average fast fluence of 1.51×10^{19} neutrons/cm^2 (>1 MeV).

Fig. 2. Charpy V-notch impact energy vs test temperature for HSSI weld 73W in the unirradiated condition and following irradiation at 288°C to an average fast fluence of 1.51×10^{19} neutrons/cm^2 (>1 MeV).

Fig. 3. Fracture toughness, K_{Jc}, vs test temperature for HSSI weld 72W in the unirradiated condition. Compact specimens up to 203.2 mm thick [8T C(T)] were tested. All results are on or above the ASME Code K_{Ic} curve.

Fig. 4. Fracture toughness, K_{Jc}, vs test temperature for HSSI weld 73W in the unirradiated condition. Compact specimens up to 203.2 mm thick [8T C(T)] were tested. A lower-bound curve to the data falls about 5°C lower in temperature than the ASME K_{Ic} curve.

Fig. 5. Fracture toughness, K_{Jc}, vs test temperature for HSSI weld 72W irradiated at 288°C to an average fast fluence of 1.5×10^{19} neutrons/cm^2 (>1 MeV). Compact specimens up to 101.6 mm thick [4T C(T)] were irradiated. The ASME K_{Ic} curve was shifted equal to the Charpy 41-J shift as required by ASTM E 185. Two cleavage pop-in values fall below the shifted curve.

Fig. 6. Fracture toughness, K_{Jc}, vs test temperature for HSSI weld 73W irradiated at 288°C to an average fast fluence of 1.5×10^{19} neutrons/cm^2 (>1 MeV). Compact specimens up to 101.6 mm thick [4T C(T)] were irradiated. The ASME K_{Ic} curve was shifted equal to the Charpy 41-J shift as required by ASTM E 185. Two cleavage fracture and four cleavage pop-in values fall below the shifted curve.

Fig. 7. Hyperbolic tangent curve fits to the unirradiated and irradiated Charpy V-notch impact energy vs temperature results for HSSI weld 72W. The bounding curves (dashed) represent one standard deviation on energy. At the 41-J level, the mean shift is about 72°C while the averaged temperature interval for the bounding curves is about ±20°C. The corresponding values at the 68-J level are 83 and ±20°C, respectively.

Fig 8. Hyperbolic tangent curve fits to the unirradiated and irradiated Charpy V-notch impact energy vs temperature results for HSSI weld 73W. The bounding curves (dashed) represent one standard deviation on energy. At the 41-J level, the mean shift is about 82°C while the averaged temperature interval for the bounding curves is about ±22°C. The corresponding values at the 68-J level are 105 and ±27°C, respectively.

Fig. 9. Cleavage fracture toughness for irradiated HSSI weld 72W comparing first pop-in events with fracture toughness results from fracture events at the same test temperature. Each datum represents one specimen. Note that temperature axis is not scaled.

List of Figures (Continued)

Fig. 10. Results of linear regressions for the fracture toughness results from HSSI weld 72W. A linearized three-parameter exponential model with the intercept fixed at 36.48 MPa•√m was used; the plot shows the mean fits as well as the one standard deviation bounding curves.

Fig. 11. Results of linear regressions for the fracture toughness results from HSSI weld 73W. A linearized three-parameter exponential model with the intercept fixed at 36.48 MPa•√m was used; the plot shows the mean fits as well as the one standard deviation bounding curves.

Fig. 12. Results of linear regressions for the fracture toughness results from HSSI welds 73W. The results are plotted vs the normalized temperature, $T - RT_{NDT}$. The temperature offset of the irradiated data reflect the greater temperature shift for the fracture toughness than that for the Charpy data, while the increasing offset with increasing fracture toughness reflects the reduced slope of the curve for the irradiated data.

Fig. 13. Results of fracture toughness vs precleavage stable ductile tearing for unirradiated HSSI weld 73W. The data from 1T through 8T compact specimens form a resistance curve with no apparent size effects.

Fig. 14. Fracture toughness, K_{Jc}, vs test temperature normalized to the RT_{NDT} for the combined results from unirradiated HSSI welds 72W and 73W. The curves are the results of linear regressions using a simple exponential model and show transition temperatures increasing with specimen size.

Fig. 15. Fracture toughness, K_{Jc}, vs $(T - T_o)$ for all the combined data from HSSI welds 72W and 73W, where T_o is the temperature corresponding to 100 MPa•√m using the Wallin procedure. The curve labeled Wallin is the 63.2 percentile curve, $K_o = 31 + 77*\exp[0.019(T - T_o)]$, from Wallin while the curve labeled $K_{0.05}$ is the five percentile curve from the ORNL analysis using the Wallin procedure. All data shown were adjusted for size using the Wallin procedure.

Fig. 16. Fracture toughness, K_{Jc}, vs test temperature for irradiated HSSI weld 72W. The ASME K_{Ic} curve for the unirradiated data is shown as is the same curve after shifting it upward in temperature equal to the Charpy 41-J shift. The curves labeled 1, 2, and 3 represent the ASME curve shifted by the indicated criterion, where Margin is 15.6°C. The K_{Ia} curve represent the ASME K_{Ia} curve shifted by the Charpy 41-J shift. The $K_{0.05}$ curve is the five percentile curve for all the HSSI 72W and 73W combined data using the Wallin procedure.

Fig. 17. Fracture toughness, K_{Jc}, vs test temperature for irradiated HSSI weld 73W. The ASME K_{Ic} curve for the unirradiated data is shown as is the same curve after shifting it upward in temperature equal to the Charpy 41-J shift. The curves labeled 1, 2, and 3 represent the ASME curve shifted by the indicated criterion, where Margin is 15.6°C. The K_{Ia} curve represent the ASME K_{Ia} curve shifted by the Charpy 41-J shift. The $K_{0.05}$ curve is the five percentile curve for all the HSSI 72W and 73W combined data using the Wallin procedure.

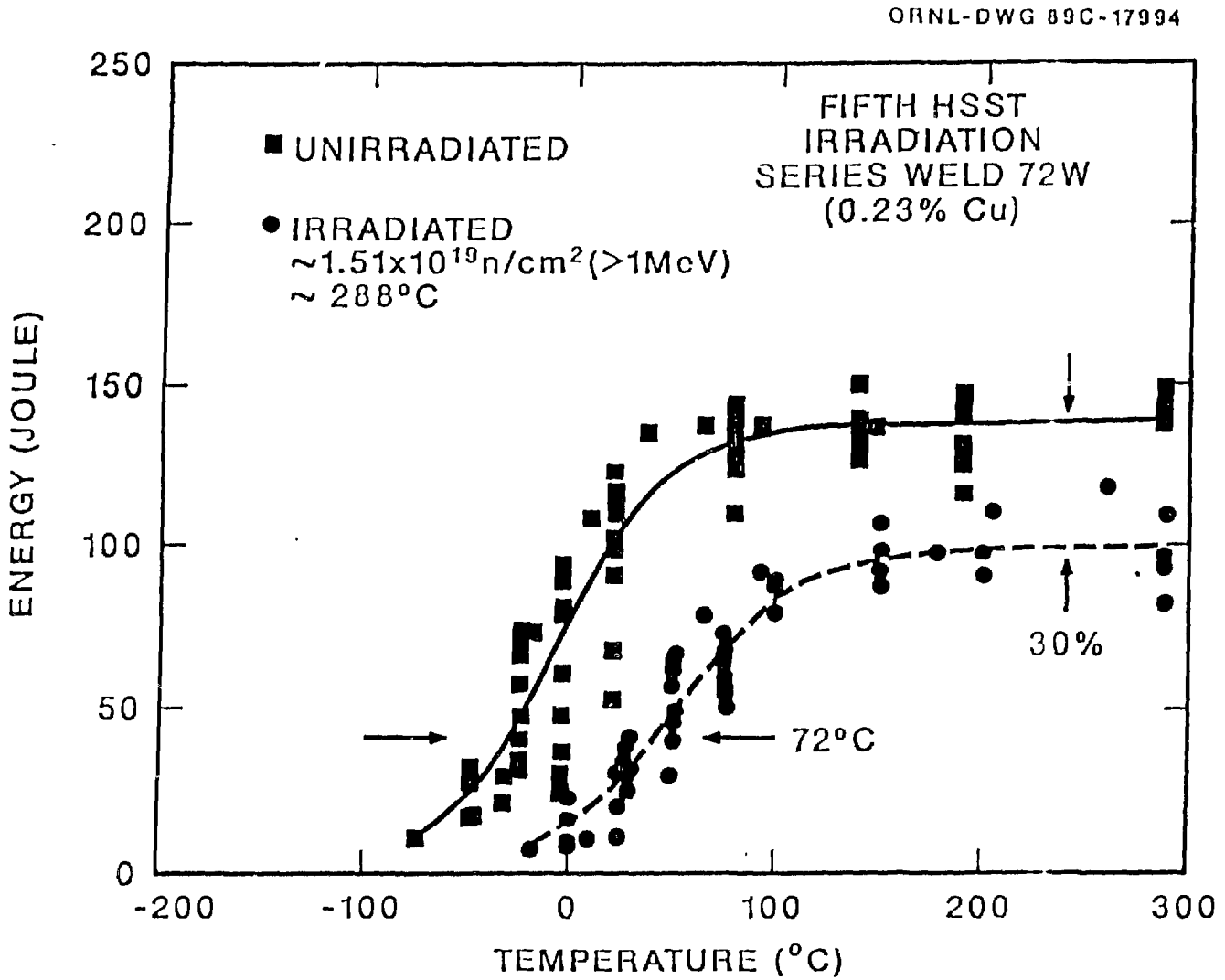

Fig. 1. Charpy V-notch impact energy vs test temperature for HSSI weld 72W in the unirradiated condition and following irradiation at 288°C to an average fast fluence of 1.51×10^{19} neutrons/cm^2 (>1 MeV).

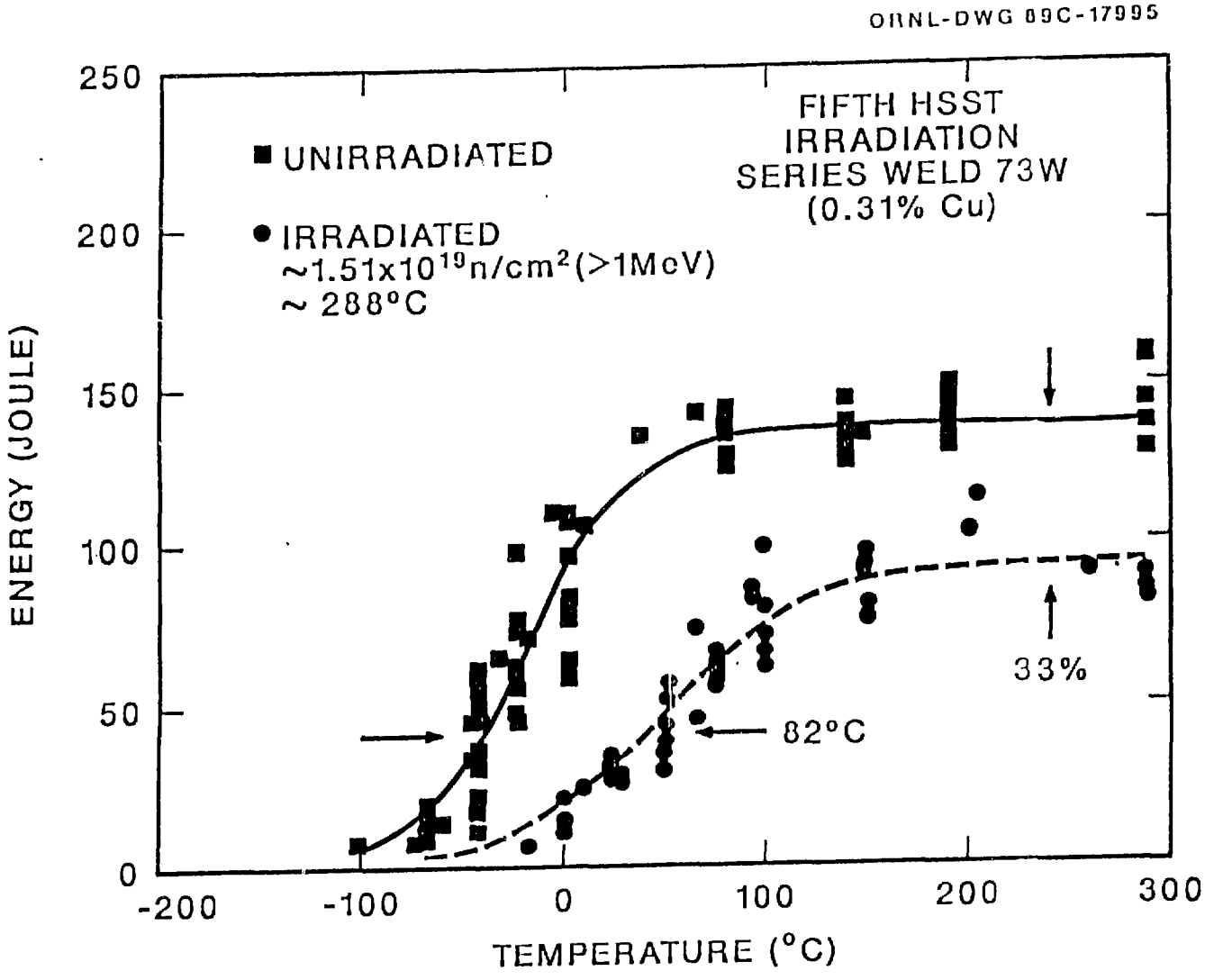

Fig. 2. Charpy V-notch impact energy vs test temperature for HSSI weld 73W in the unirradiated condition and following irradiation at 288°C to an average fast fluence of 1.51×10^{19} neutrons/cm^2 (>1 MeV).

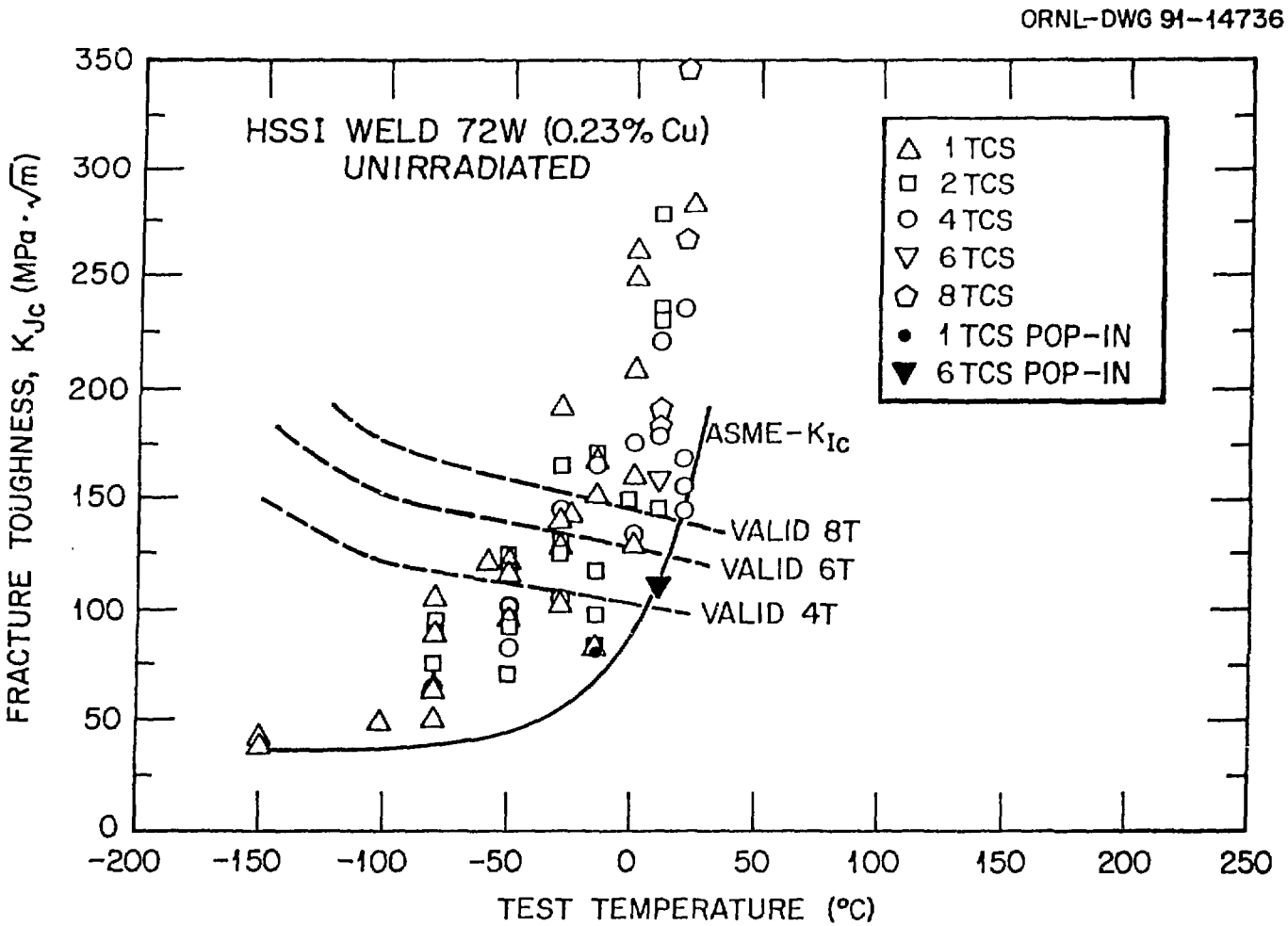

Fig. 3. Fracture toughness, K_{Jc}, vs test temperature for HSSI weld 72W in the unirradiated condition. Compact specimens up to 203.2 mm thick [8T C(T)] were tested. All results are on or above the ASME Code K_{Ic} curve.

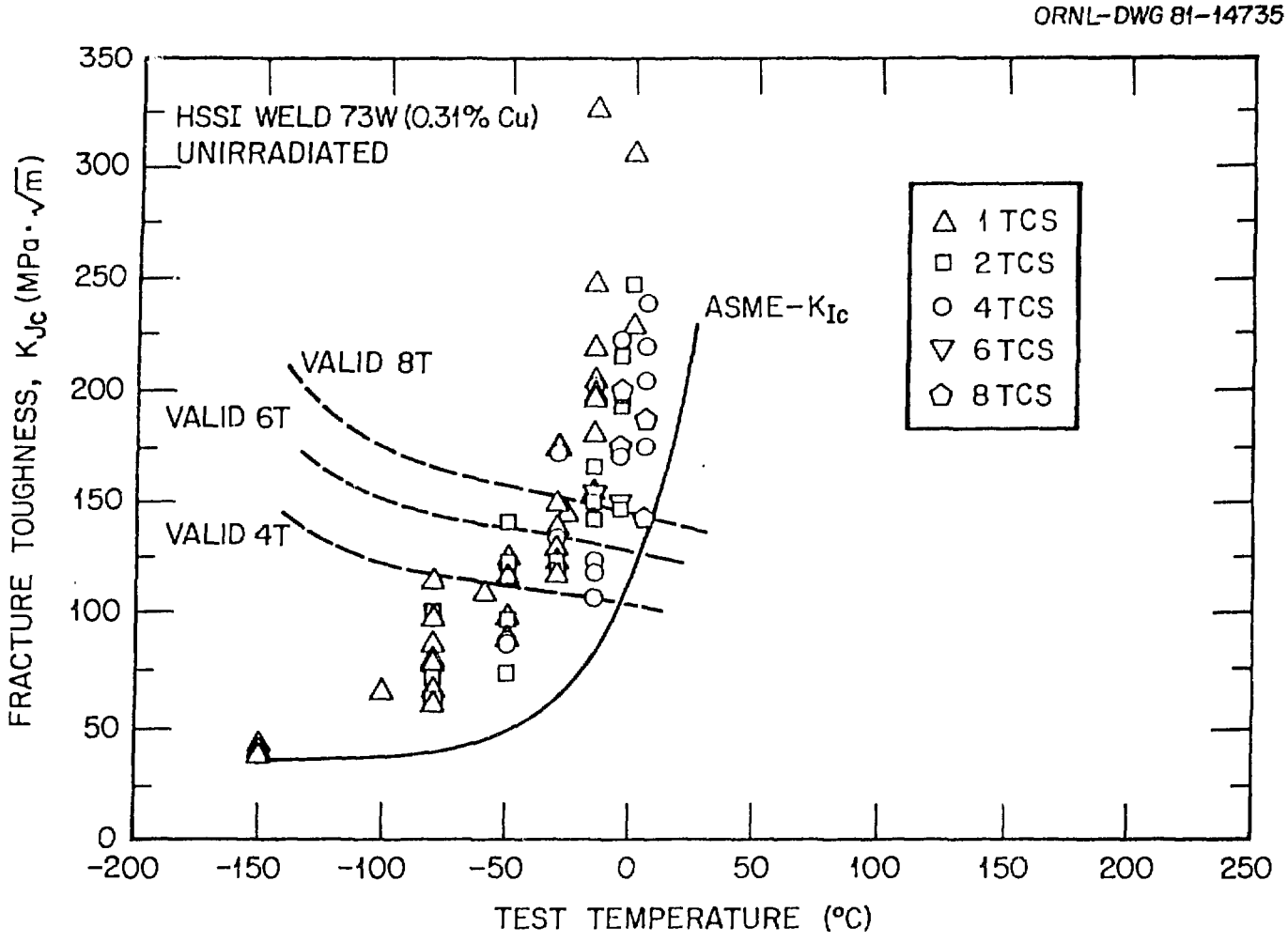

Fig. 4. Fracture toughness, K_{Jc}, vs test temperature for HSSI weld 73W in the unirradiated condition. Compact specimens up to 203.2 mm thick [8T C(T)] were tested. A lower-bound curve to the data falls about 5°C lower in temperature than the ASME K_{Ic} curve.

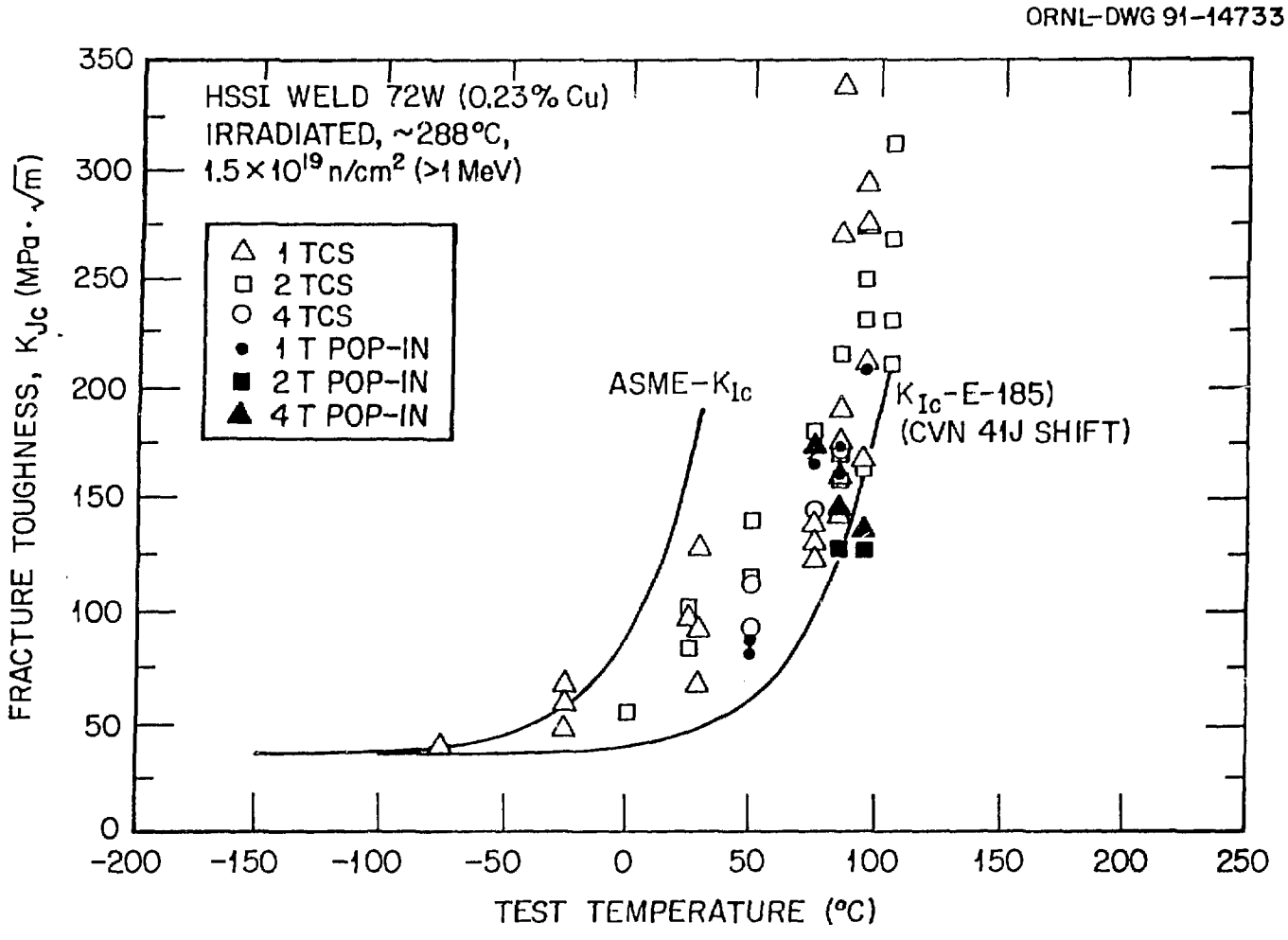

Fig. 5. Fracture toughness, K_{Jc}, vs test temperature for HSSI weld 72W irradiated at 288°C to an average fast fluence of 1.5×10^{19} neutrons/cm^2 (>1 MeV). Compact specimens up to 101.6 mm thick [4T C(T)] were irradiated. The ASME K_{Ic} curve was shifted equal to the Charpy 41-J shift as required by ASTM E 185. Two cleavage pop-in values fall below the shifted curve.

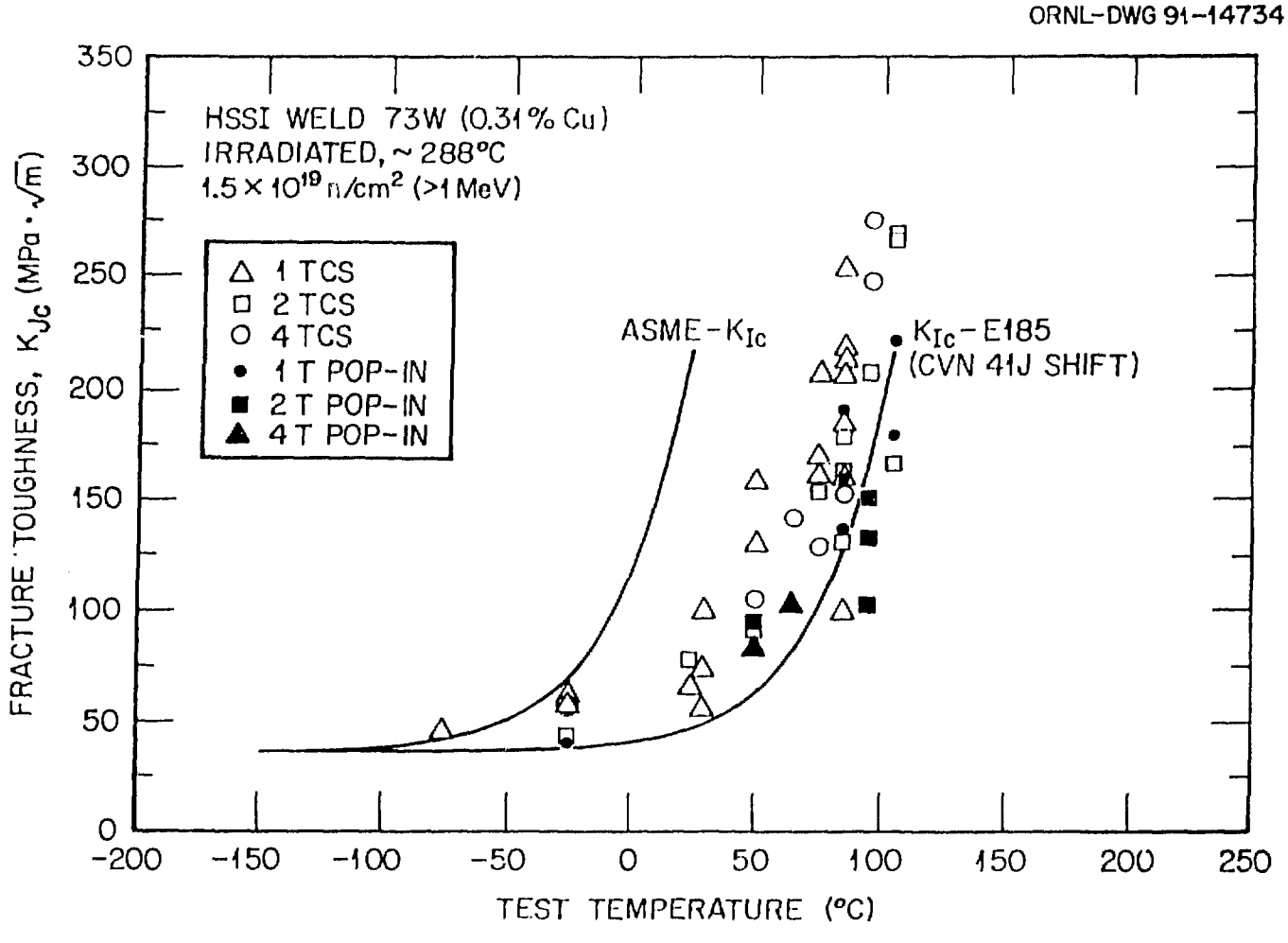

Fig. 6. Fracture toughness, K_{Jc}, vs test temperature for HSSI weld 73W irradiated at 288°C to an average fast fluence of 1.5×10^{19} neutrons/cm^2 (>1 MeV). Compact specimens up to 101.6 mm thick [4T C(T)] were irradiated. The ASME K_{Ic} curve was shifted equal to the Charpy 41-J shift as required by ASTM E 185. Two cleavage fracture and four cleavage pop-in values fall below the shifted curve.

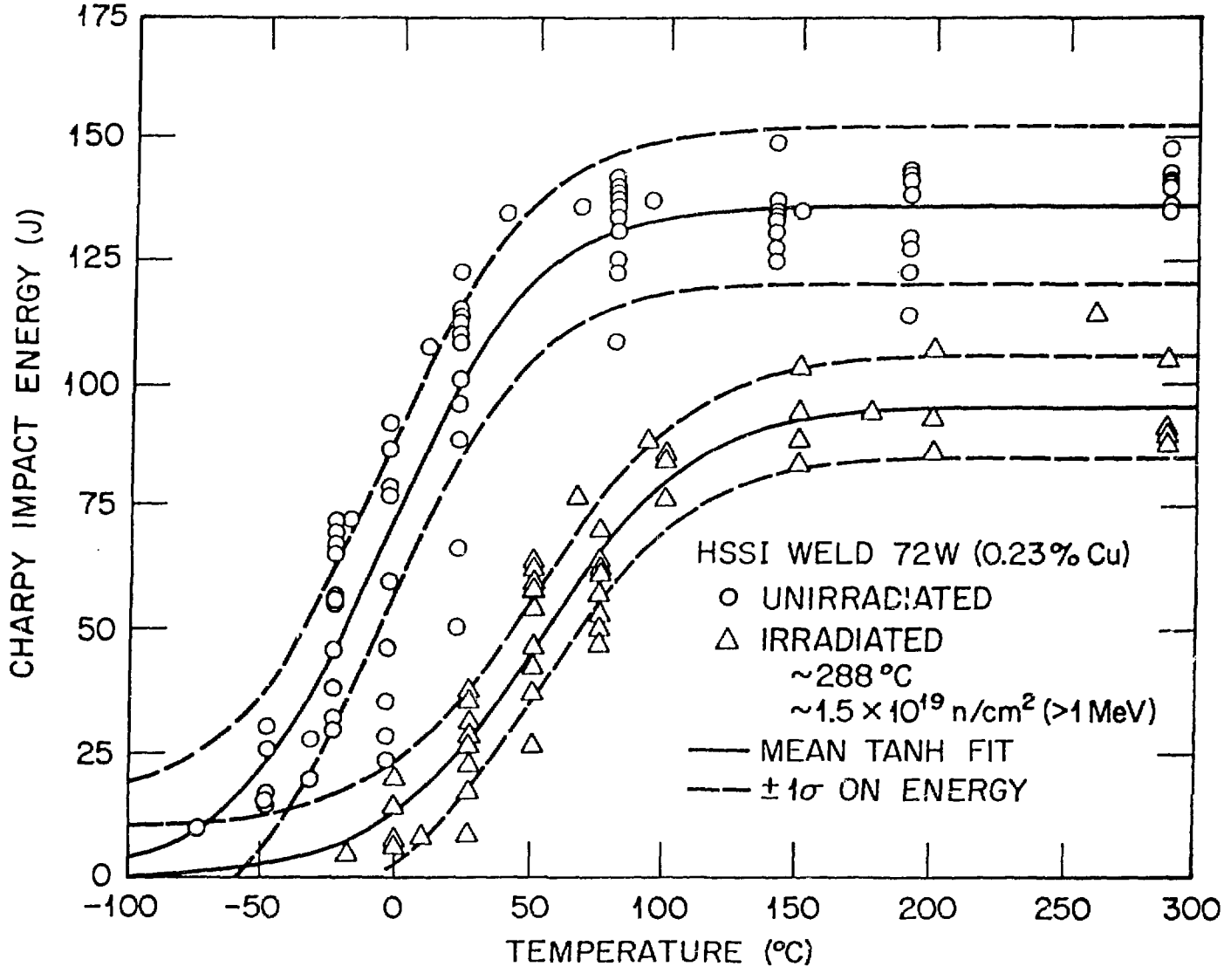

Fig. 7. Hyperbolic tangent curve fits to the unirradiated and irradiated Charpy V-notch impact energy vs temperature results for HSSI weld 72W. The bounding curves (dashed) represent one standard deviation on energy. At the 41-J level, the mean shift is about 72°C while the averaged temperature interval for the bounding curves is about ±20°C. The corresponding values at the 68-J level

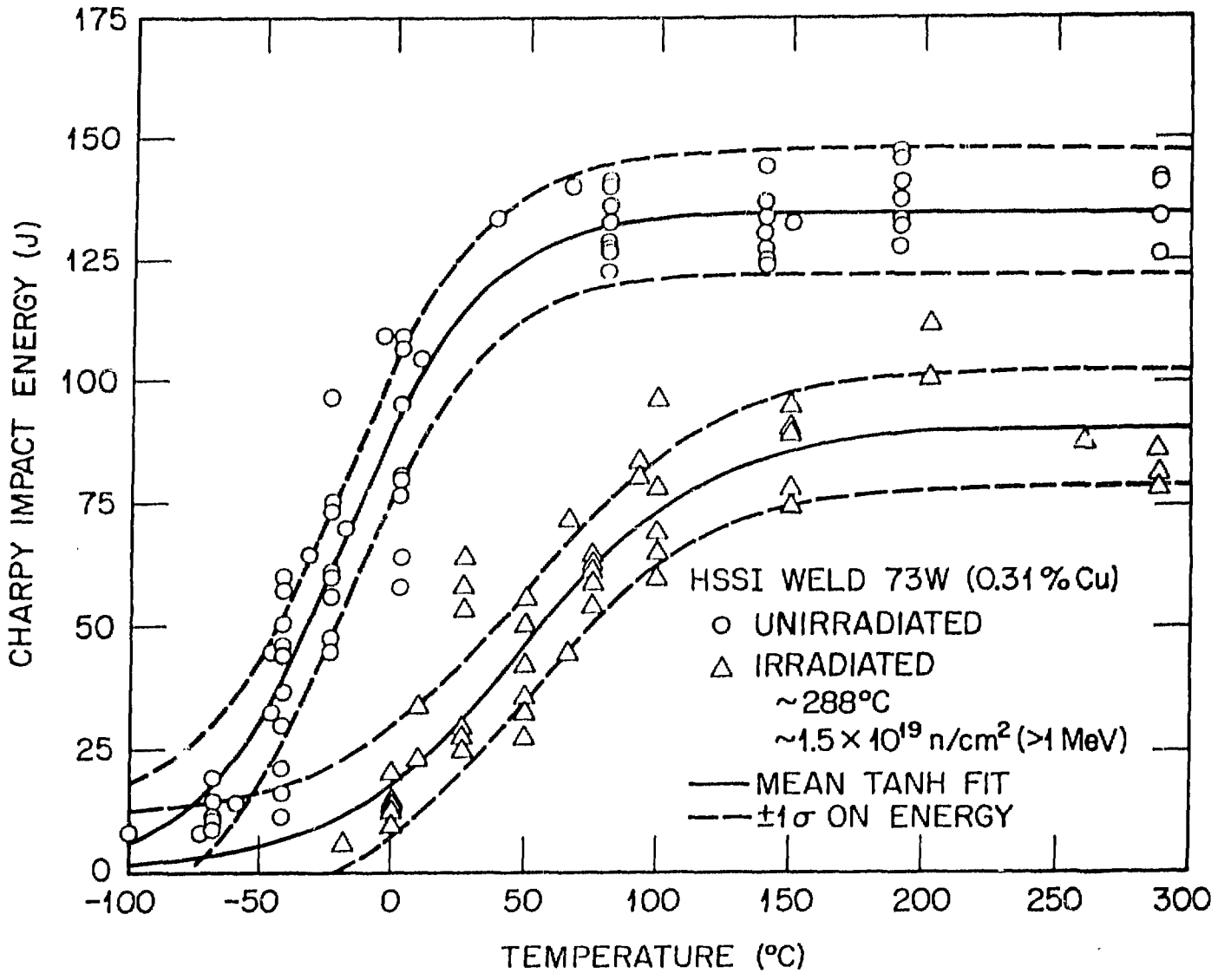

Fig. 8. Hyperbolic tangent curve fits to the unirradiated and irradiated Charpy V-notch impact energy vs temperature results for HSSI weld 73W. The bounding curves (dashed) represent one standard deviation on energy. At the 41-J level, the mean shift is about 82°C while the averaged temperature interval for the bounding curves is about ±22°C. The corresponding values at the 68-J level are 105 and ±27°C, respectively.

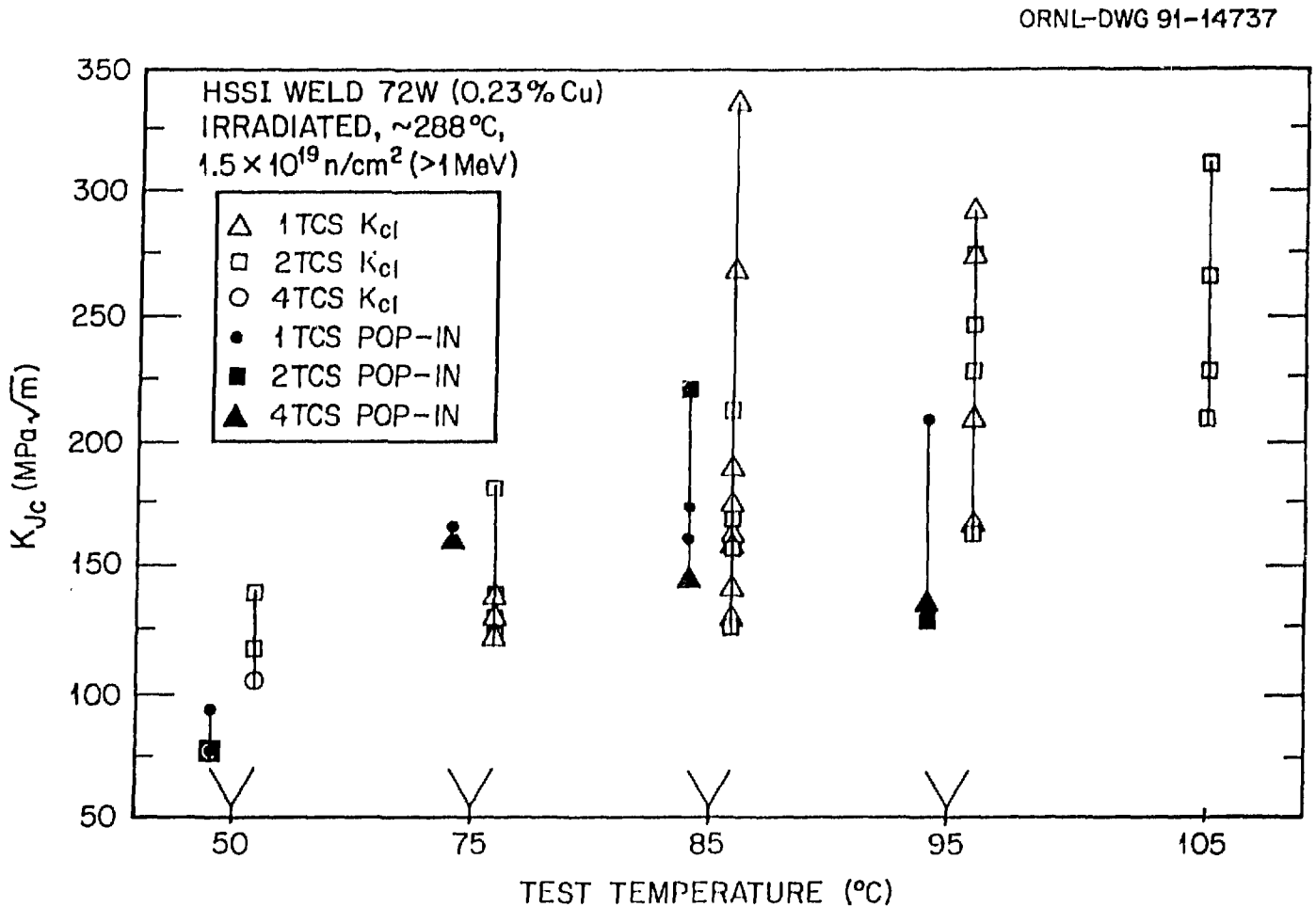

Fig. 9. Cleavage fracture toughness for irradiated HSSI weld 72W comparing first pop-in events with fracture toughness results from fracture events at the same test temperature. Each datum represents one specimen. Note that temperature axis is not scaled.

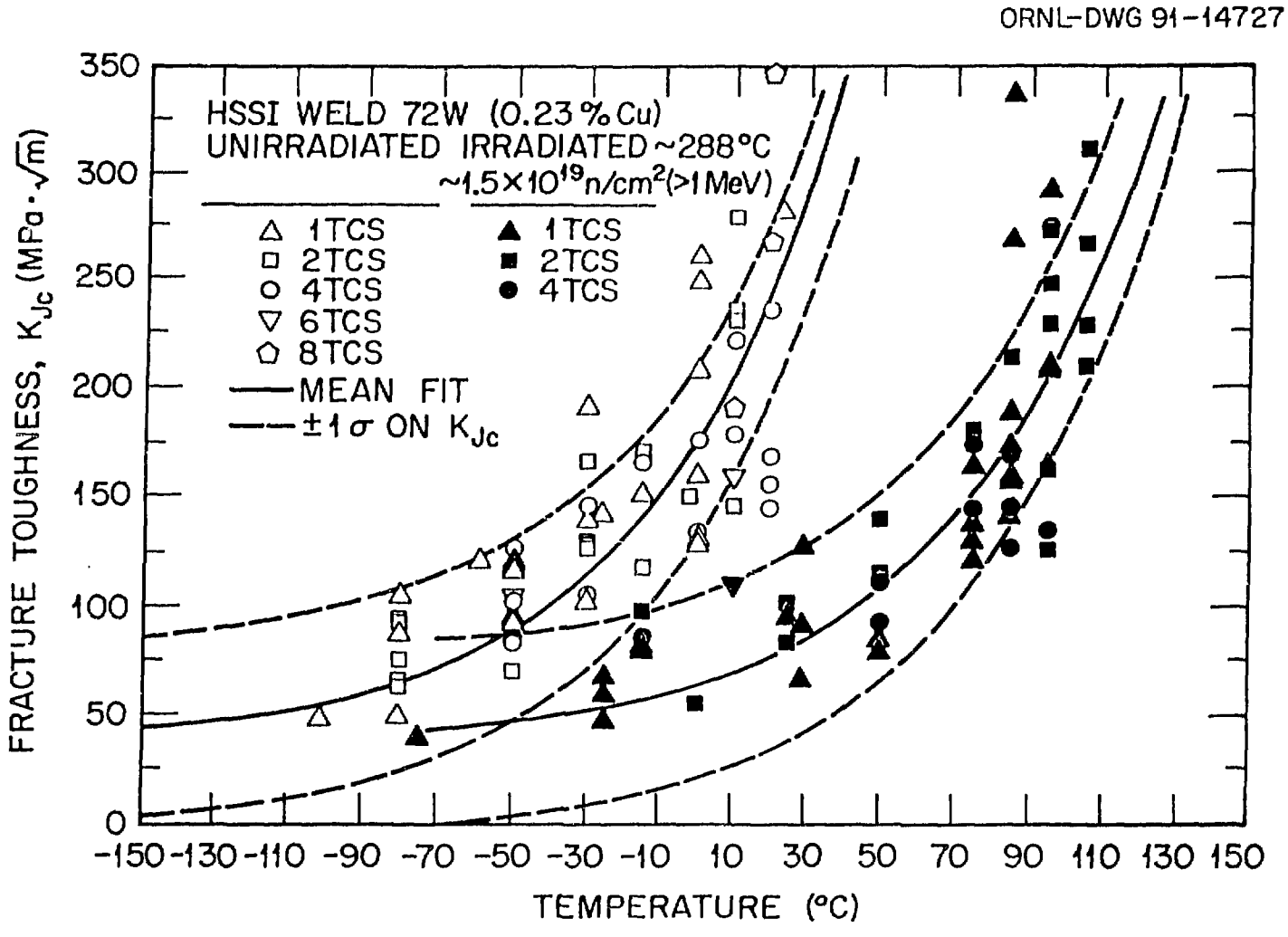

Fig. 10. Results of linear regressions for the fracture toughness results from HSSI weld 72W. A linearized three-parameter exponential model with the intercept fixed at 36.48 MPa•√m was used; the plot shows the mean fits as well as the one standard deviation bounding curves.

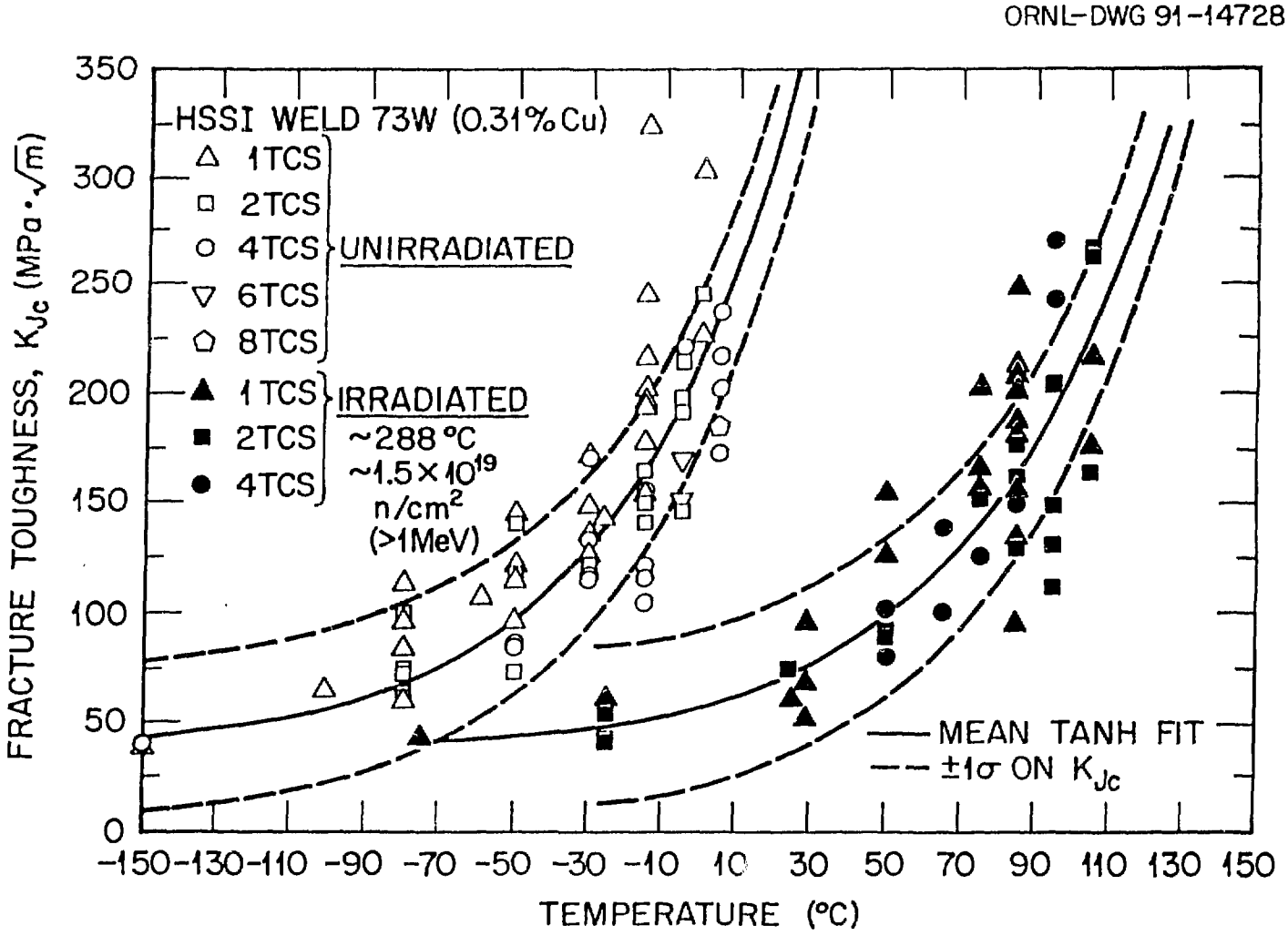

Fig. 11. Results of linear regressions for the fracture toughness results from HSSI weld 73W. A linearized three-parameter exponential model with the intercept fixed at 36.48 MPa•√m was used; the plot shows the mean fits as well as the one standard deviation bounding curves.

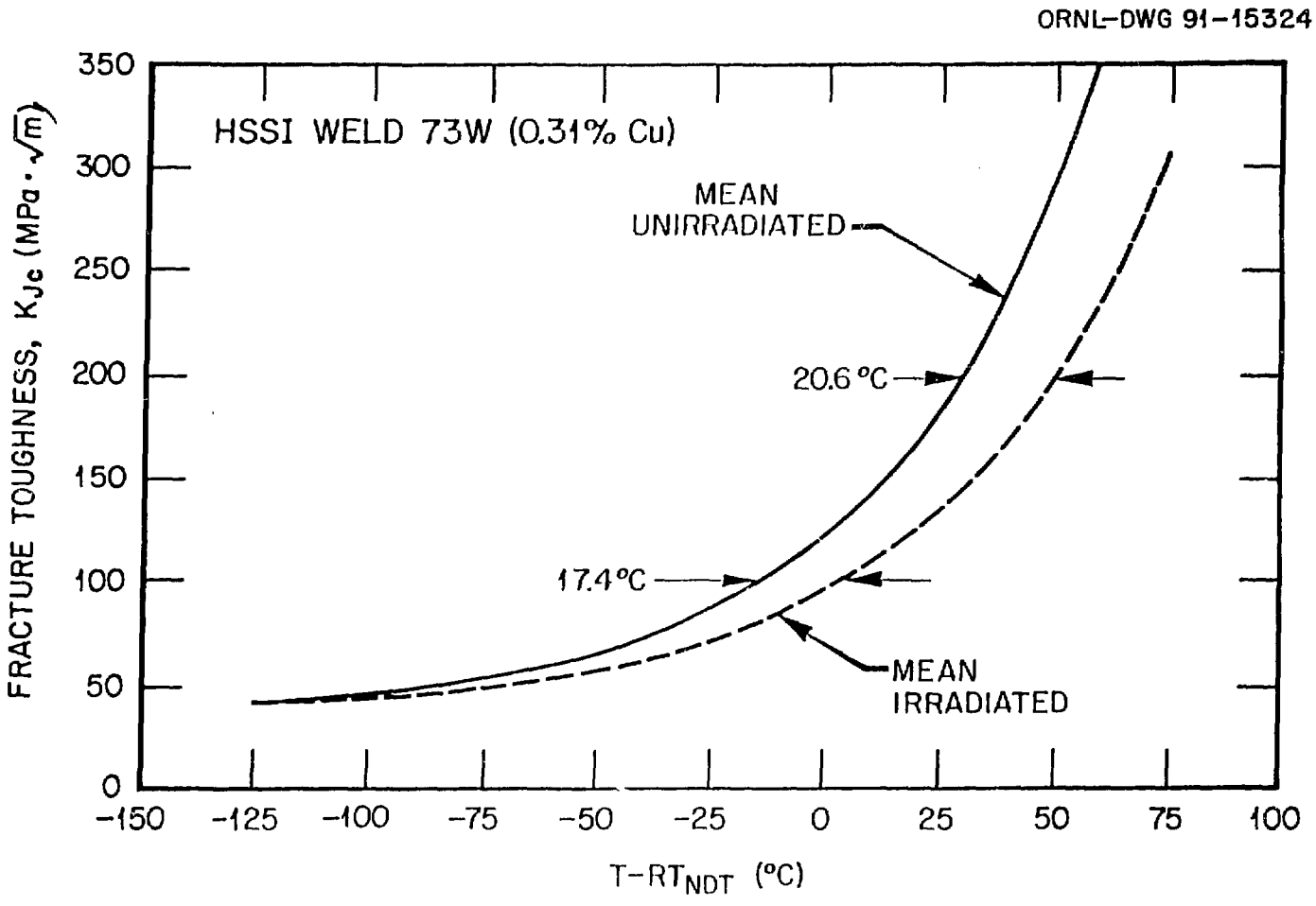

Fig. 12. Results of linear regressions for the fracture toughness results from HSSI welds 73W. The results are plotted vs the normalized temperature, T - RT_{NDT}. The temperature offset of the irradiated data reflect the greater temperature shift for the fracture toughness than that for the Charpy data, while the increasing offset with increasing fracture toughness reflects the reduced slope of the curve for the irradiated data.

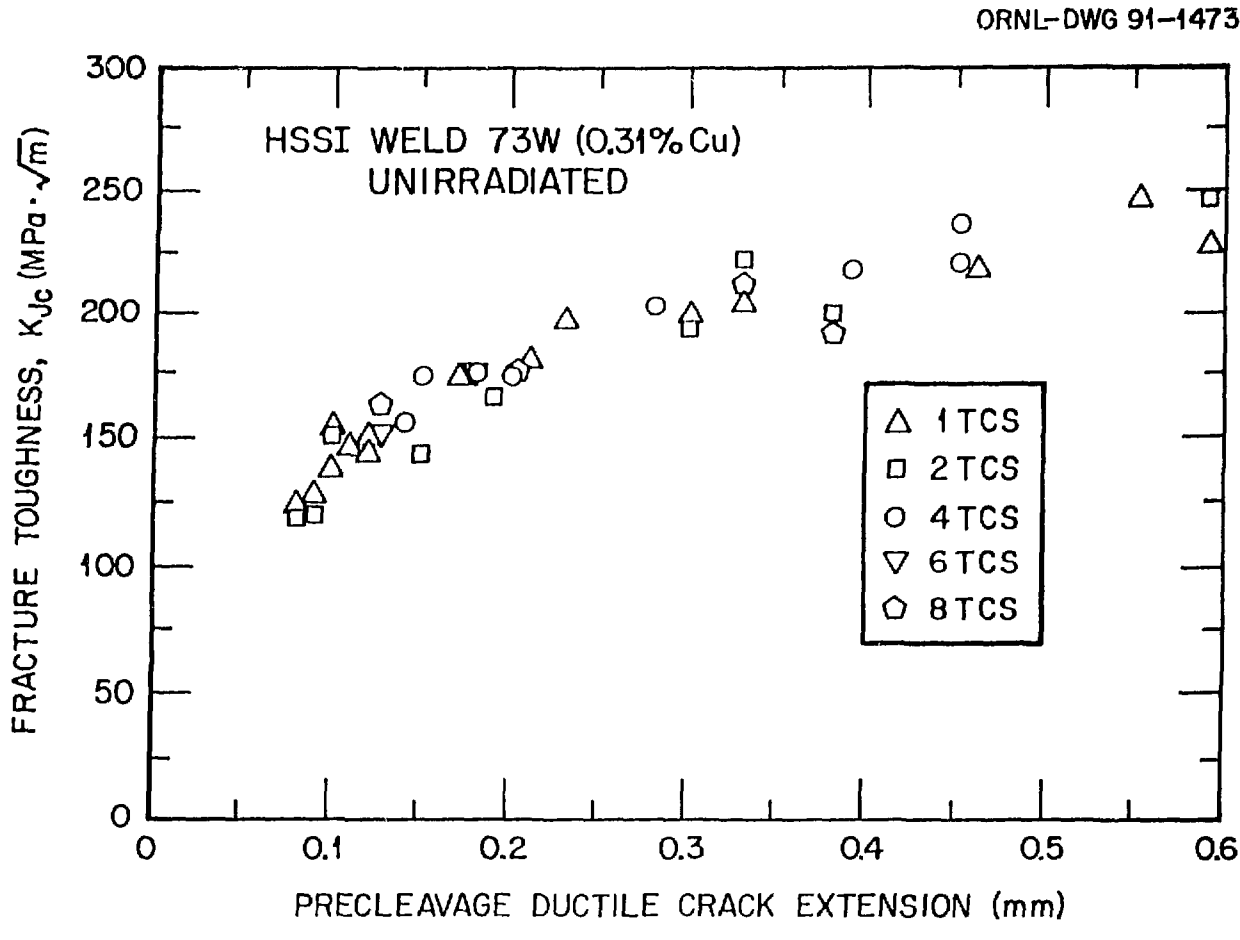

Fig. 13. Results of fracture toughness vs precleavage stable ductile tearing for unirradiated HSSI weld 73W. The data from 1T through 8T compact specimens form a resistance curve with no apparent size effects.

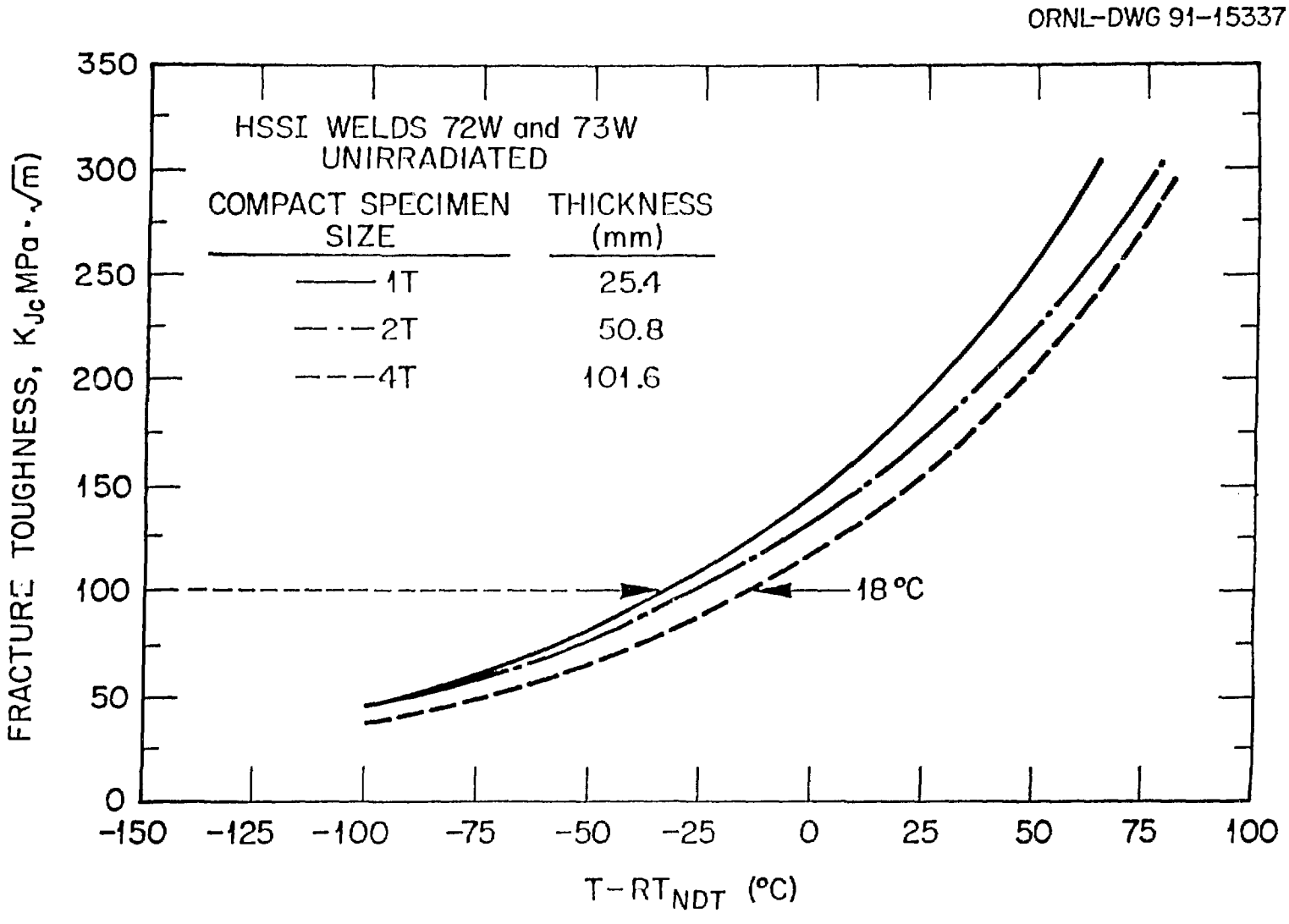

Fig. 14. Fracture toughness, K_{Jc}, vs test temperature normalized to the RT_{NDT} for the combined results from unirradiated HSSI welds 72W and 73W. The curves are the results of linear regressions using a simple exponential model and show transition temperatures increasing with specimen size.

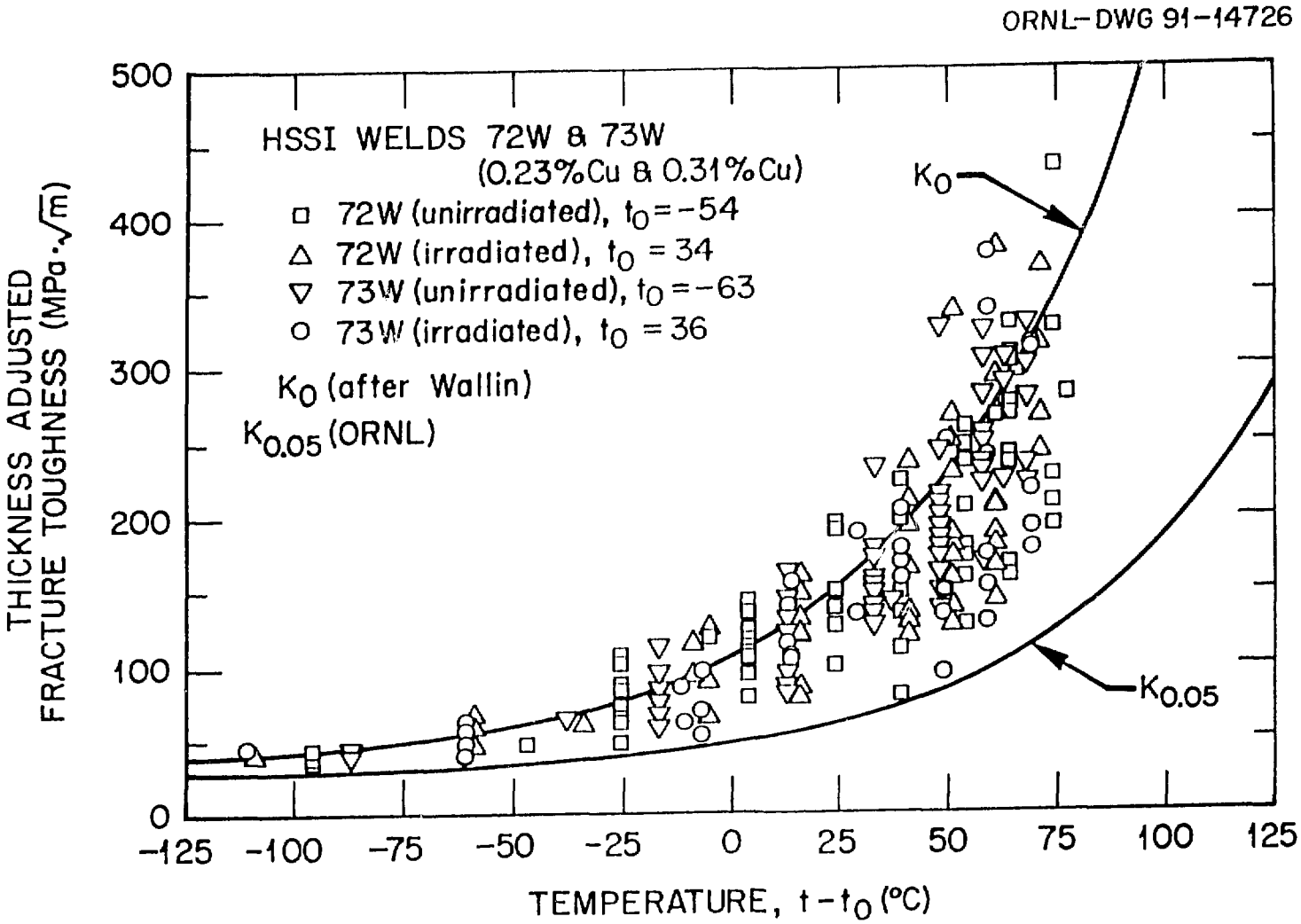

Fig. 15. Fracture toughness, K_{Jc}, vs $(T - T_o)$ for all the combined data from HSSI welds 72W and 73W, where T_o is the temperature corresponding to 100 MPa•√m using the Wallin procedure. The curve labeled Wallin is the 63.2 percentile curve, $K_o = 31 + 77*\exp[0.019(T - T_o)]$, from Wallin while the curve labeled $K_{0.05}$ is the five percentile curve from the ORNL analysis using the Wallin procedure. All data shown were adjusted for size using the Wallin procedure.

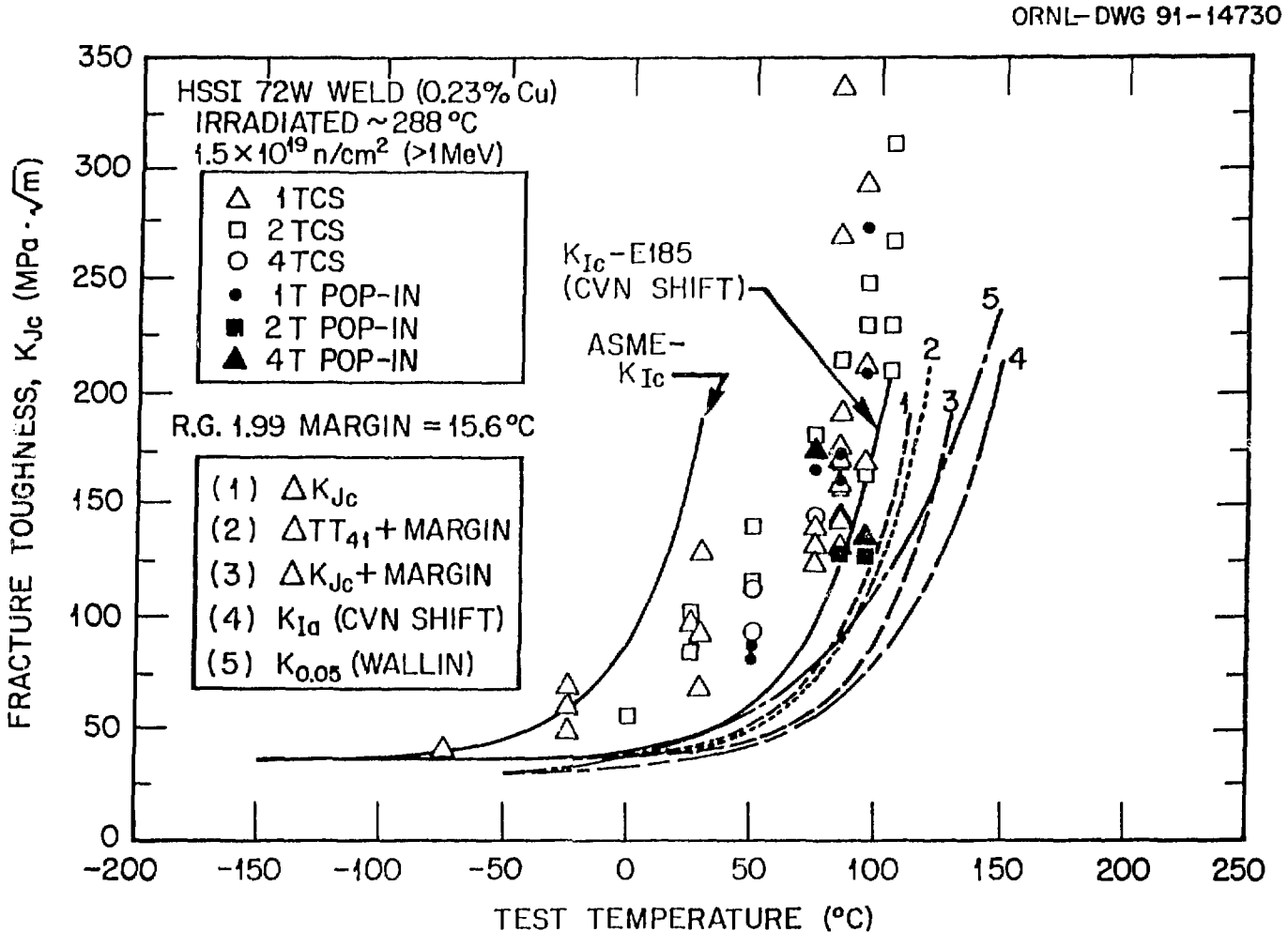

Fig. 16. Fracture toughness, K_{Jc}, vs test temperature for irradiated HSSI weld 72W. The ASME K_{Ic} curve for the unirradiated data is shown as is the same curve after shifting it upward in temperature equal to the Charpy 41-J shift. The curves labeled 1, 2, and 3 represent the ASME curve shifted by the indicated criterion, where Margin is 15.6°C. The K_{Ia} curve represent the ASME K_{Ia} curve shifted by the Charpy 41-J shift. The $K_{0.05}$ curve is the five percentile curve for all the HSSI 72W and 73W combined data using the Wallin procedure.

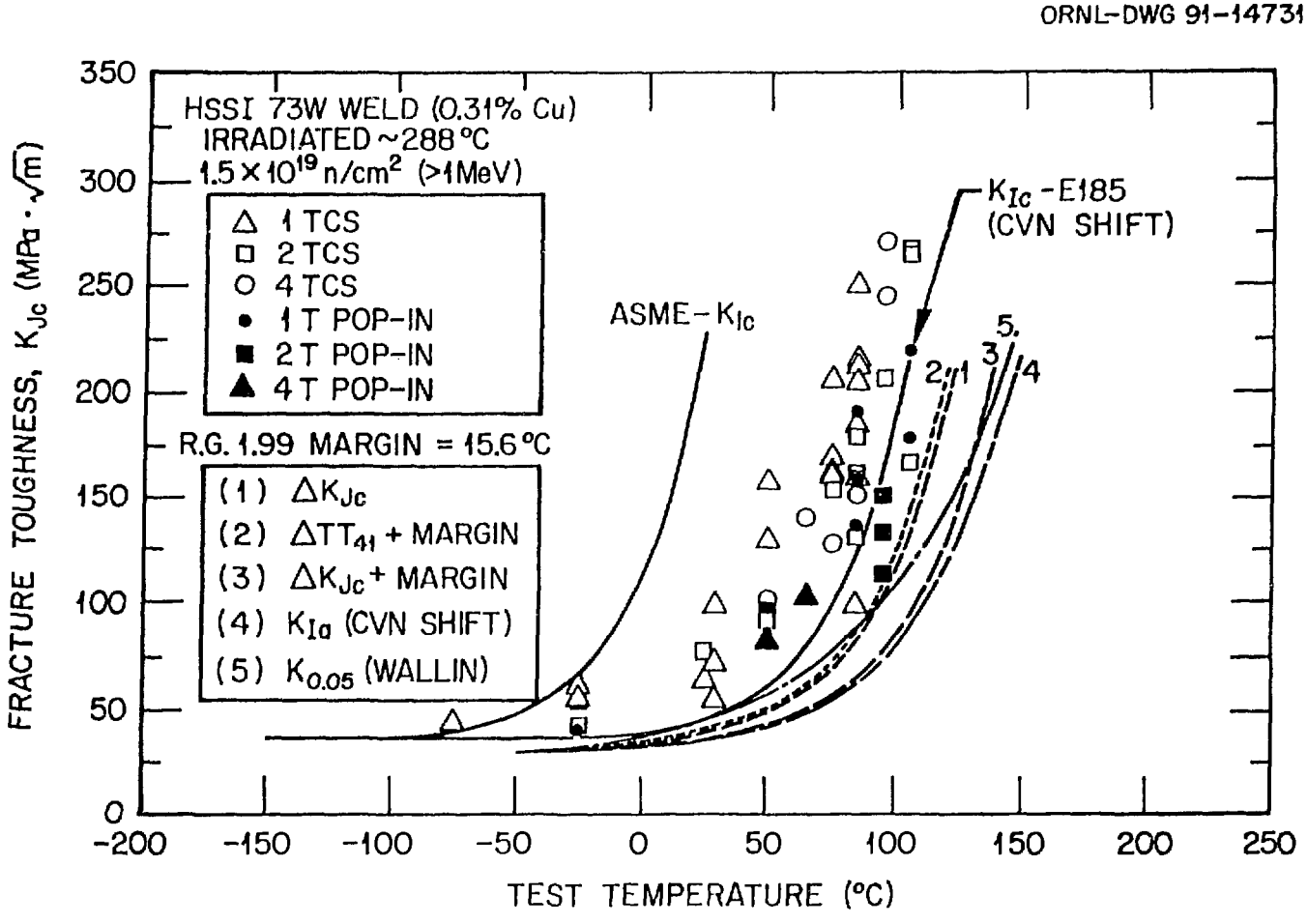

Fig. 17. Fracture toughness, K_{Jc}, vs test temperature for irradiated HSSI weld 73W. The ASME K_{Ic} curve for the unirradiated data is shown as is the same curve after shifting it upward in temperature equal to the Charpy 41-J shift. The curves labeled 1, 2, and 3 represent the ASME curve shifted by the indicated criterion, where Margin is 15.6°C. The K_{Ia} curve represent the ASME K_{Ia} curve shifted by the Charpy 41-J shift. The $K_{.05}$ curve is the five percentile curve for all the HSSI 72W and 73W combined data using the Wallin procedure.